Global and Planetary Change 131 (2015) 174–191

Contents lists available at ScienceDirect

Global and Planetary Change

journal homepage: www.elsevier.com/locate/gloplacha

A micropalaeontological perspective on export productivity, oxygenation and temperature in NE Atlantic deep-waters across Terminations I and II

Patrick Grunert [a,b,*], Luke Skinner [c], David A. Hodell [c], Werner E. Piller [b]

[a] Department of Earth and Planetary Sciences, Rutgers University, 610 Taylor Road, Piscataway, NJ 08854-8066, USA
[b] Institute for Earth Sciences, University of Graz, NAWI Graz, Heinrichstrasse 26, 8010 Graz, Austria
[c] Godwin Laboratory for Palaeoclimate Research, Department of Earth Sciences, University of Cambridge, Cambridge CB2 3EQ, United Kingdom

ARTICLE INFO

Article history:
Received 15 February 2015
Received in revised form 29 May 2015
Accepted 2 June 2015
Available online 5 June 2015

Keywords:
Benthic foraminifera
Glacial terminations
Iberian margin
Taphonomy
Multiproxy records
IODP Site U1385

ABSTRACT

Census counts of benthic foraminifera were studied from the SW Iberian Margin to reconstruct past changes in deep-water hydrography across Terminations I and II. Detailed benthic faunal data (>125 μm size-fraction) allow us to evaluate the limitations imposed by taphonomic processes and restricted size-fractions. The comparison of recent (mudline) and fossil assemblages at IODP Site U1385 indicates the quick post-mortem disintegration of shells of astrorhizoid taxa (~80% of the present-day fauna), resulting in impoverished fossil assemblages. While the application of quantitative proxy methods is problematic under these circumstances, the fossil assemblages can still provide a qualitative palaeoenvironmental signal that, while most fully expressed in the 125–212 μm size-fraction, is nonetheless also expressed to some degree in the >212 μm size-fraction.

Variations in the benthic foraminiferal assemblages reveal information about changing organic matter supply, deep-water oxygenation and temperature. MIS 2 is generally characterized by an elevated trophic state and variable oxic conditions, with oxygenation minima culminating in the Younger Dryas (YD) and Heinrich Stadials (HS) 1, 2 and 3. Low oxic conditions coincide with decreased water-temperature and lower benthic $\delta^{13}C$, pointing to the strong influence of a southern sourced water-mass during these periods. HS 1 is the most extreme of these intervals, providing further evidence for a severe temporary reduction or even shutdown of AMOC. With the inception of MIS 1, organic matter supply reduced and a better ventilated deep-water environment bathed by NEADW is established.

For Termination II, clear indications of southern-sourced water are limited to the early phase of HS 11. During the latter part of HS 11, the deep-water environment seems to be determined by strongly increased supply of organic matter, potentially explaining the decoupling of benthic $\delta^{13}C$ and Mg/Ca records of earlier studies as a phytodetritus effect on the carbon isotope signal. However, the presence of a warm, nutrient-rich and poorly oxygenated water-mass cannot be ruled out. With the inception of interglacial MIS 5e trophic conditions are reduced and ventilation by NEADW increases.

1. Introduction

Deep-sea sediments of the SW Iberian Margin show a remarkable sensitivity to climate change on orbital and sub-orbital time scales and have stimulated a number of landmark studies in palaeoclimatic and palaeoceanographic research on glacial/interglacial cycles (see Voelker and de Abreu, 2011, for a review). Shackleton et al. (2000) demonstrated that a signal of interhemispheric phasing is preserved in the sediments: changes in $\delta^{18}O$ of planktonic foraminifera follow the Greenland ice core record, whereas the $\delta^{18}O$ record of benthic foraminifera resembles variations in the Antarctica temperature signal. Furthermore, the area is situated at the southern edge of the ice rafting debris (IRD) belt, and melting icebergs reached the western Iberian Margin during Heinrich and Greenland stadials of the last glacial cycle and during ice-rafting events (IREs) of preceding glacial periods (Hodell et al., 2008). Finally, the relative proximity to the continent allows for good pollen preservation and correlation of marine and terrestrial records (Margari et al., 2014 and references therein). The western Iberian Margin is thus a unique place to study Quaternary climate, and there is an ever-growing amount of geochemical, geophysical and micropalaeontological data available for the area that allows detailed insights in the hydrography of surface, intermediate and deep waters for the past 1.4 Myrs (see e.g., Shackleton et al., 2000; Skinner and Elderfield, 2007; Voelker and de Abreu, 2011; Hodell et al., 2013a, 2013b; Margari et al., 2014 and references therein).

Proxy methods based on benthic foraminiferal assemblages have been applied to track changes in deep-water hydrography along the

* Corresponding author at: Department of Earth and Planetary Sciences, Rutgers University, 610 Taylor Road, Piscataway, NJ 08854-8066, USA.
E-mail addresses: patrick.grunert@rutgers.edu, patrick.grunert@uni-graz.at (P. Grunert).

http://dx.doi.org/10.1016/j.gloplacha.2015.06.002

western Iberian Margin since the last glacial maximum (Caralp, 1987; Baas et al., 1998; Schönfeld and Zahn, 2000; Schönfeld et al., 2003). The exclusive focus on shells >250 μm ensured the time-efficient acquisition of quantitative data at high stratigraphic resolution as well as methodological consistency between studies. However, the restriction of the analysis to coarser size-fractions resulted in low numbers of specimens, an impoverished faunal inventory and loss of small-sized index species. The latter results in the potential loss of important palaeoenvironmental information (Schröder et al., 1987; Schönfeld et al., 2003; Schönfeld, 2012). In addition, taphonomic processes may bias the composition of any fossil assemblage and remain a major concern with all micropalaeontological proxy methods (Jorissen et al., 2007). The standing stock of benthic foraminifera in the study area shows a strong dominance of agglutinating foraminifera, in strong contrast to Holocene and Pleistocene assemblages that rarely contain agglutinated tests (Caralp, 1987; Baas et al., 1998; Phipps et al., 2012; Expedition 339 Scientists, 2013). This decline in agglutinated shells within the uppermost sediment column reflects taphonomic disintegration (Schröder, 1988; Kuhnt et al., 2000), a potential problem that was not addressed in previous studies.

Mudline and core samples recovered from IODP Site U1385 provide a way to address these issues (Expedition 339 Scientists, 2013). In this study, we present census counts of ~34,000 shells of benthic foraminifera across the last and penultimate glacial/interglacial transitions from four deep-sea cores on the southwestern Iberian Margin. Two types of quantitative data-sets are compared and integrated: a low-resolution data-set that represents the complete foraminiferal inventory >125 μm, and a high-resolution data-set focusing on the most abundant taxa >212 μm. This two-fold approach allows for 1) the assessment of the limitations imposed on benthic foraminiferal proxy records by taphonomy and the reliance on coarser size-fractions; and 2) the reconstruction of relative changes in bottom water oxygenation, organic matter availability and deep water temperature and, ultimately, changes in deep-water circulation across Terminations I and II.

2. Regional setting

The studied cores include: U1385D-1H (37°34.28′N, 10°7.56′W; 2584 m water depth), U1385E-3H (37°34.28′N, 10°7.57′W; 2589 m), MD99-2334 K (37°48′N, 10°10′W; 3146 m) and MD01-2444 (37°33.88′N, 10°8.34′W; 2656 m). They have all been recovered from an elevated spur on the upper slope of the southwestern Iberian Margin (Fig. 1; Hodell et al., 2013a). At present, these sites are bathed in northward re-circulating Northeast Atlantic Deep Water (NEADW; temperature: 2–10 °C; salinity: 35–36 psu), a derivative of North Atlantic Deep Water (NADW; Van Aken, 2000; Voelker and de Abreu, 2011). NEADW is sourced from Lower Deep Water (LDW), Labrador Sea Water (LSW), Iceland–Scotland Overflow Water (ISOW), and, to a minor extent, Mediterranean Outflow Water (MOW) (Van Aken, 2000). Warm (10–12 °C) and highly saline (>36 psu) MOW overlies NEADW at depths <1500 m. Below 4000 m, NEADW is underlain by cold (2 °C) and low saline (<35 psu) LDW, which is derived from Antarctic Bottom Water (AABW; Van Aken, 2000; Hernandez-Molina et al., 2011).

Over the past 400 kyrs, oscillations in the Atlantic meridional overturning circulation (AMOC) and thus, antagonistic changes in the export of southward NADW and northward AABW, have significantly altered deep-water hydrography in the area across glacial/interglacial and stadial/interstadial cycles (Hodell et al., 2013a). The severe reduction or even shut down of AMOC during Heinrich and Greenland stadials resulted in a significant shoaling of the Glacial North Atlantic Intermediate Water (GNAIW)/AABW boundary, the increased influence of cold, more poorly ventilated southern sourced waters, and increased nutrient availability in the study area (Baas et al., 1998; Sarnthein et al., 2000; Shackleton et al., 2000; Williamowski and Zahn, 2000; Schönfeld et al., 2003; Skinner et al., 2003; Skinner and Shackleton, 2006; Skinner and Elderfield, 2007; Voelker and de Abreu, 2011). While the depth of AABW shoaled, an enhanced MOW core settled deeper in the water column during at least some of the Heinrich stadials (Schönfeld and Zahn, 2000; Voelker and de Abreu, 2011).

3. Material and methods

3.1. Sample material and data-sets

Four quantitative data-sets of benthic foraminifera across Terminations I and II have been acquired from the southwestern Iberian Margin cores for this study. 1 cm-thick slices of sediment have been collected from half sections of the studied cores. After washing the samples over a >63 μm sieve, benthic foraminiferal shells of the targeted size-fractions were picked from the dried residues, determined and counted (see Appendix A for taxonomy). Fragments of foraminiferal shells have been counted as individual specimens. The data-sets group in two types:

3.1.1. Low-resolution records of benthic foraminifera >125 μm

These data-sets, collected from cores U1385D-1H and U1385E-3H of IODP Expedition 339, consist of a limited number of samples (25) due to time constraints but represent a quantitative record of the entire microfaunal inventory >125 μm. Foraminiferal shells from size-fractions 125–212 μm and >212 μm have been counted separately to evaluate potential biases on the interpretation of the high-resolution records >212 μm. In some samples (1.12, 2.3, 2.5, 2.6, 2.8–2.10), the size-fraction 125 μm–212 μm contained a very high amount of foraminiferal shells and has been subdivided into smaller portions by using a standard microsplitter to facilitate counting.

The analysed data-sets for Termination I (14 samples) and Termination II (11 samples) come from the intervals between 0.2 m and 3.62 m (mcd) and 21.02 m to 23.13 m (mcd), respectively, of the U1385D/E shipboard splice. Depths at these sites are always indicated as metres composite depth (mcd). The identification of the Younger Dryas (YD), Heinrich Stadial (HS) 1 and HS 11 is based on δ^{18}O- and XRF-data (Fig. 2; Hodell et al., 2013b).

3.1.2. High-resolution records of benthic foraminifera >212 μm

These data-sets (188 samples) have been acquired from cores MD99-2334 K and MD01-2444 (Skinner, PhD Thesis, 2004). Due to low total numbers of foraminifera, in particular in samples from MIS 1 and MIS 5e, the focus is placed on the most abundant taxa at each site that allows for the analysis of a greater number of samples (Fatela and Taborda, 2002; Schönfeld et al., 2003). Other benthic foraminiferal taxa that show minor abundances have not been differentiated.

The high-resolution data-set representing Termination I consists of 143 samples taken at average intervals of 4 cm (range: 2–12 cm) from the upper part (4–466 cm corrected depth) of core MD99-2334 K. The identification of the YD and HS 1, 2, and 3 has been adopted from Skinner et al. (2003) and Skinner and Shackleton (2006). Depth refers to the corrected depth scale of Skinner and McCave (2003) at this site.

The high-resolution data-set for the penultimate glaciation and Termination II has been acquired from core MD01-2444. Forty-five samples have been taken with an average spacing of 2 cm (range: 1–3 cm) from the depth interval between 2100 cm and 2202 cm. The identification of HS 11 is based on Skinner and Shackleton (2006) and Hodell et al. (2013a).

3.2. Mudline samples

To account for a potential taphonomic bias on the fossil assemblages, the low-resolution data-sets are compared to benthic foraminiferal assemblages >125 μm from the mudline cores of IODP Sites U1385B, U1385C and U1385E. These samples represent the unconsolidated sediment collected from the top of the first core at each site. Although an

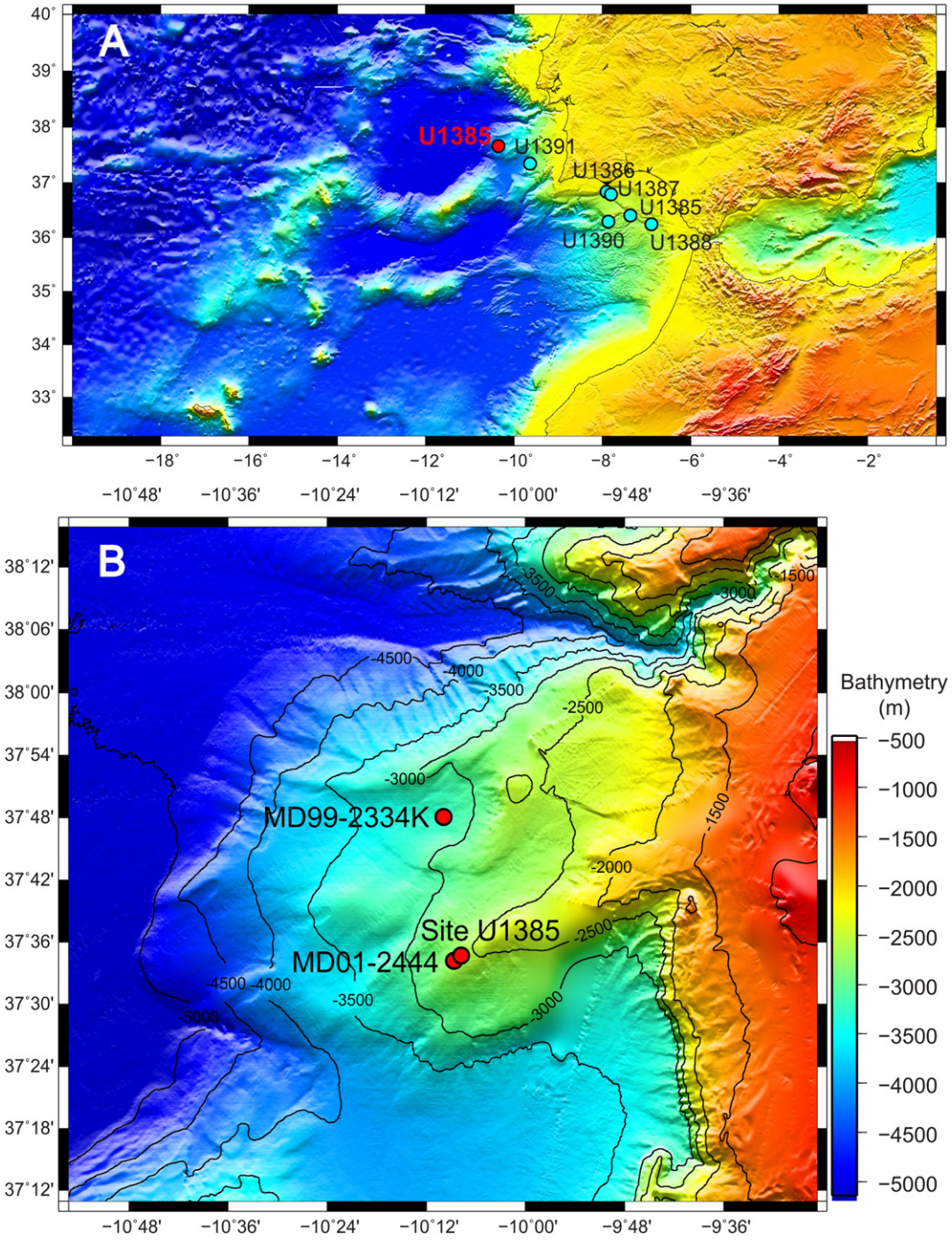

Fig. 1. Location of the studied drill-sites at the southwestern Iberian Margin. (A) Sites U1385–U1391 of IODP Expedition 339. (B) IODP Site U1385 and sites MD99-2334 K and MD01-2444.

unspecified amount of sediment containing foraminifera is unavoidably lost during the APC (advanced piston coring) drilling process, the integration of mudline samples from several sites should provide an approximation of the recent time-averaged live and dead assemblage. The samples have been stained with Rose Bengal after collection, and the presence of stained benthic foraminifera (*Astrorhiza granulosa*, Astrorhizoidea indet., *Triloculina tricarinata*, *Bulimina alazanensis*, *Pyrulina angusta*) confirms that the mudline assemblages represent the recent fauna (live and dead) of the uppermost centimetres of seafloor sediment. Stained and unstained tests have been combined for the present analysis.

3.3. Palaeoenvironmental analysis

We apply a suite of methods to the foraminiferal census counts that consider taphonomic effects and allow a qualitative assessment of palaeoceanographic changes in the study area. For a detailed discussion of the proxy methods the reader is referred to Section 5.1 of the Discussion.

Multivariate statistics are the basis for the interpretation of faunal changes in the low-resolution data sets. To process the large amount of census counts, the software PAST 2.17 has been used for statistical analyses (Hammer et al., 2001; Hammer, 2012). Cluster analysis

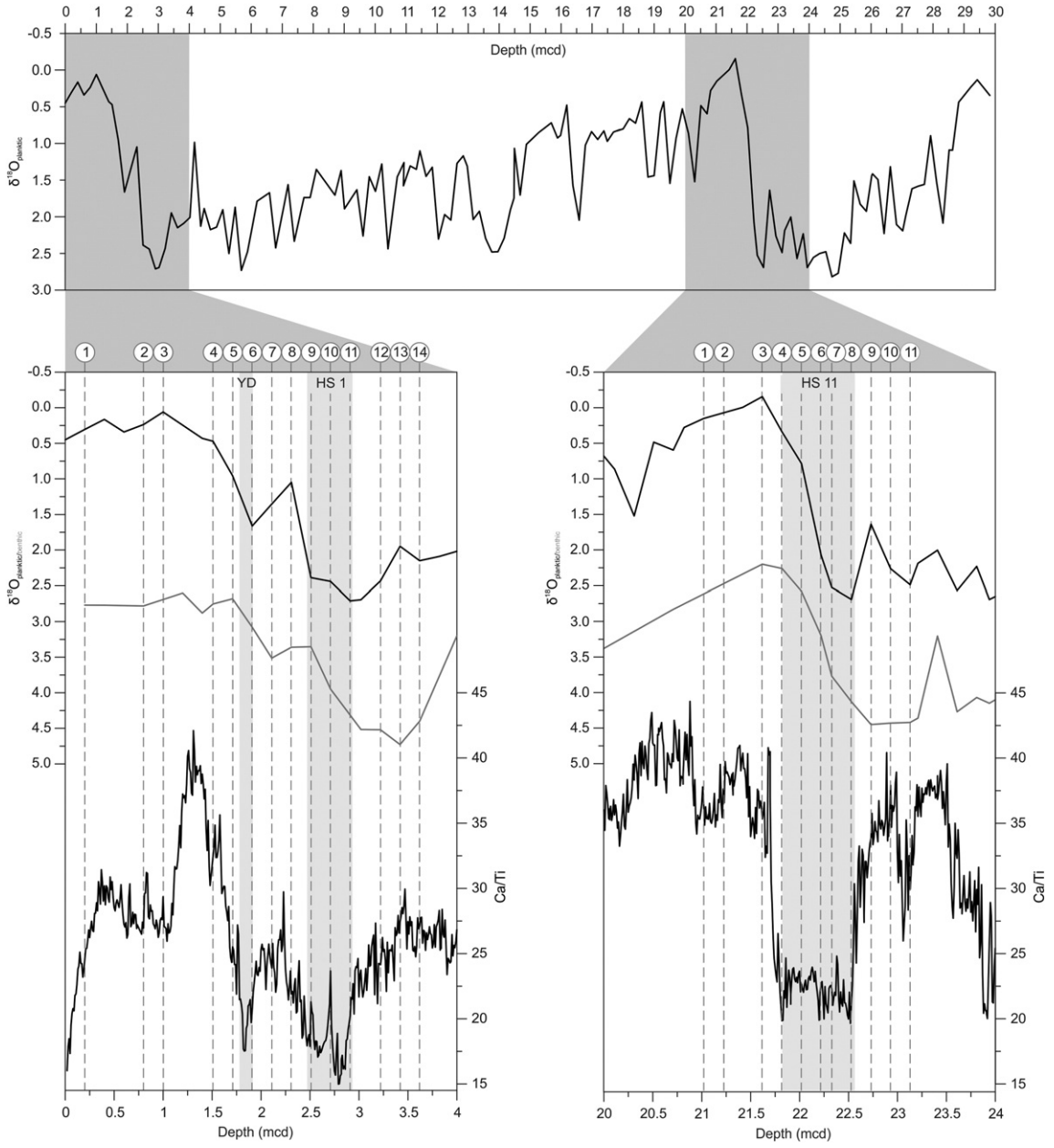

Fig. 2. Proxy records used for the identification of Terminations I and II as well as the Younger Dryas, Heinrich 1 and Heinrich 11 stadials (light grey) in the studied intervals (dark grey) of IODP Cores U1385D-1H and U1385E-3H. $\delta^{18}O$- and Ca/Ti-records from Hodell et al. (2013b). Circled numbers indicate sample locations.

(Paired-group algorithm, Euclidean distance measure) and non-metrical multidimensional scaling (nMDS; Euclidean distance measure) were performed to identify groups of samples based on similarities in their composition. A Similarity Percentage (SIMPER) analysis has been conducted to identify those taxa that primarily contribute to the differences between groups of samples revealed by cluster analysis and nMDS.

We further follow the approach of Schönfeld (2001) and Jorissen et al. (2007) and apply the abundances of deep infaunal taxa adapted to low oxic conditions (*Chilostomella* spp., *Globobulimina* spp.) as a qualitative proxy for extremely depressed oxygenation levels. The combined abundances of intermediate (*Melonis barleeanum*) and deep infaunal taxa are used to identify mesotrophic conditions (Jorissen, 2003). The abundances of miliolid shells are used as indicators of oligotrophic and comparably well-ventilated environments (Kaiho, 1999). A modified concept of BFAR (Herguera and Berger, 1991) will be introduced to assess export productivity.

4. Results

A total of ~34,000 benthic foraminiferal shells (>212 μm: ~25,000; 125–212 μm: ~9000) have been picked and counted, and >220 taxa have been determined in the low resolution data-sets. Relative abundances are shown in Figs. 3, 4 and 9, results from multivariate statistical analysis are presented in Figs. 5–8, the most important taxa are depicted on Plate 1. Tables with census counts and abundance data for all sites are available as supplementary data files (Supplementary Tables 1–5).

4.1. U1385D-1H — low resolution record of Termination I

4.1.1. >125 μm

The number of benthic foraminifera/g (18–50/g; A = 33/g, σ = 10/g) shows an overall decrease. High abundance values during MIS 2 abruptly decrease with the onset of HS 1 and remain low thereafter. This trend is mainly determined by hyaline shells (16–43/g; A = 26/g, σ = 9/g) as

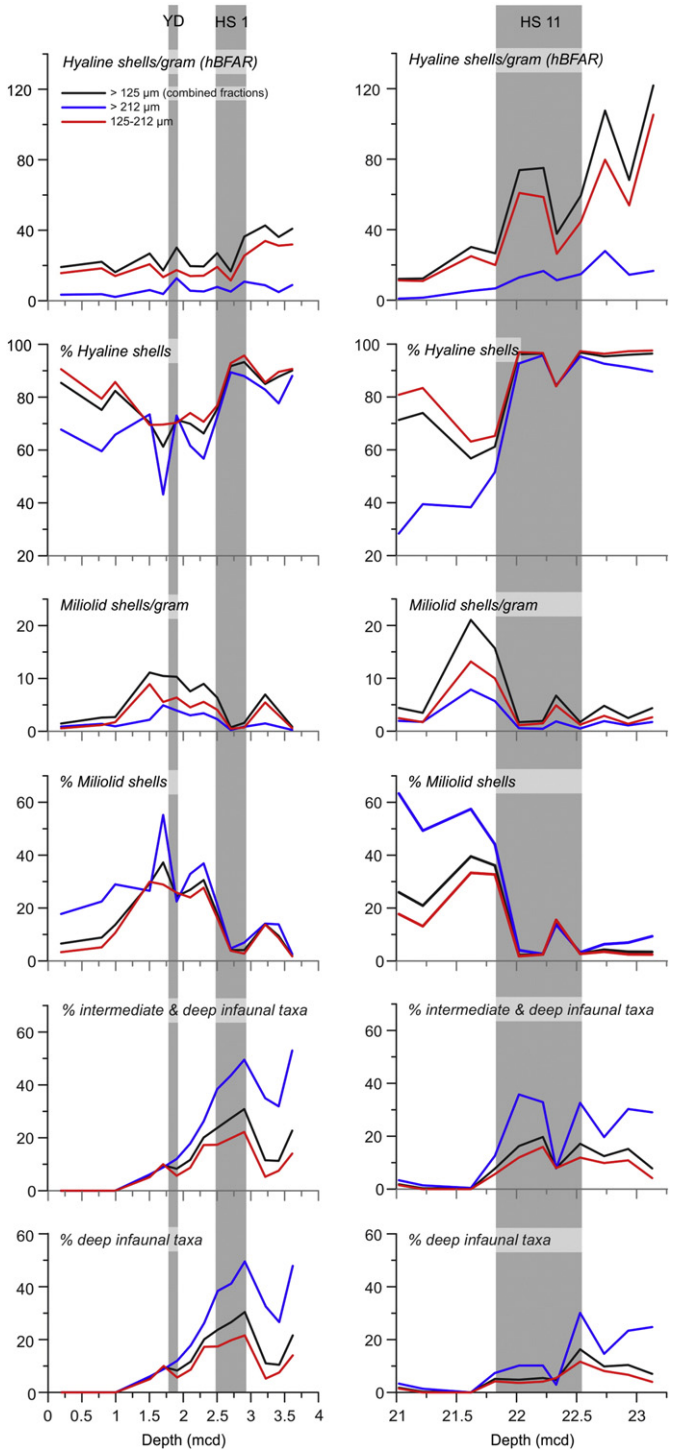

Fig. 3. Abundances of benthic foraminiferal shell types and microhabitat groups of different size-fractions in the studied intervals of IODP Site U1385. Black ≥ 125 µm (combined fractions); red = 125–212 µm; blue ≥ 212 µm. See text for a detailed discussion.

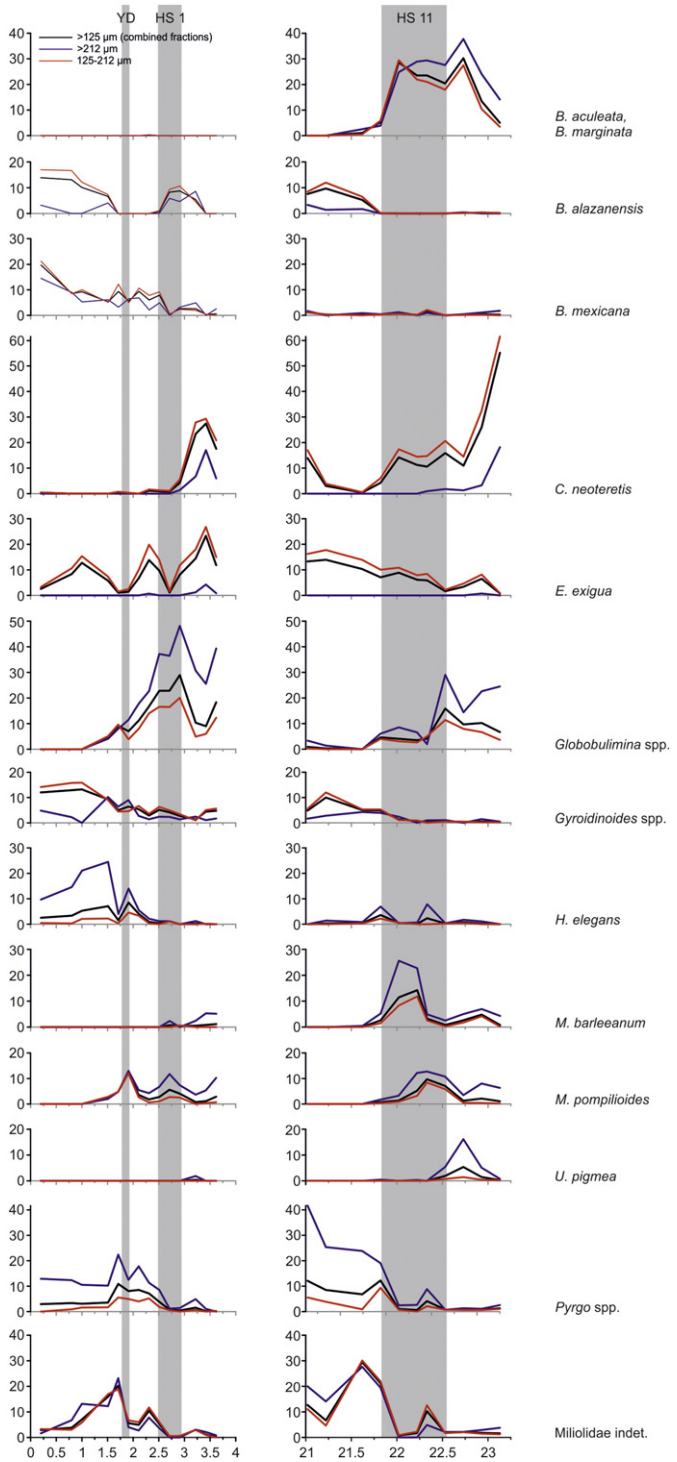

Fig. 4. Abundances of selected benthic foraminiferal taxa in different size-fractions across Terminations I (left) and II (right) at IODP Site U1385. Black ≥ 125 µm (combined fractions); red = 125–212 µm; blue ≥ 212 µm.

miliolid (1–11/g; A = 5/g, σ = 4/g) and agglutinated shells (0–5/g; A = 1/g, σ = 1/g) are represented in considerably lower numbers (Fig. 3; Supplementary Table 1).

Prominent changes in the assemblages are reflected in opposite patterns of hyaline (61–93%; A = 79%, σ = 10%) and miliolid shells (2–37%; A = 16, σ = 11%). Assemblages with *Cassidulina neoteretis* and *Epistominella exigua* as most common species during MIS 2 are replaced by assemblages with *Globobulimina* spp., *B. alazanensis* and *Melonis pompilioides* during HS 1 (Fig. 4; Supplementary Table 2). The Bølling-Allerød interstadial (BAIS) is characterized by an increase in miliolid shells, mainly represented by fragments (many of them cf. *Pyrgo*), together with *Pyrgo* spp., *Triloculina elongotricarinata* and *Sigmoilopsis schlumbergeri*, that continues with a minor decrease during the YD to the inception of MIS 1. At the same time, *Globobulimina* spp.

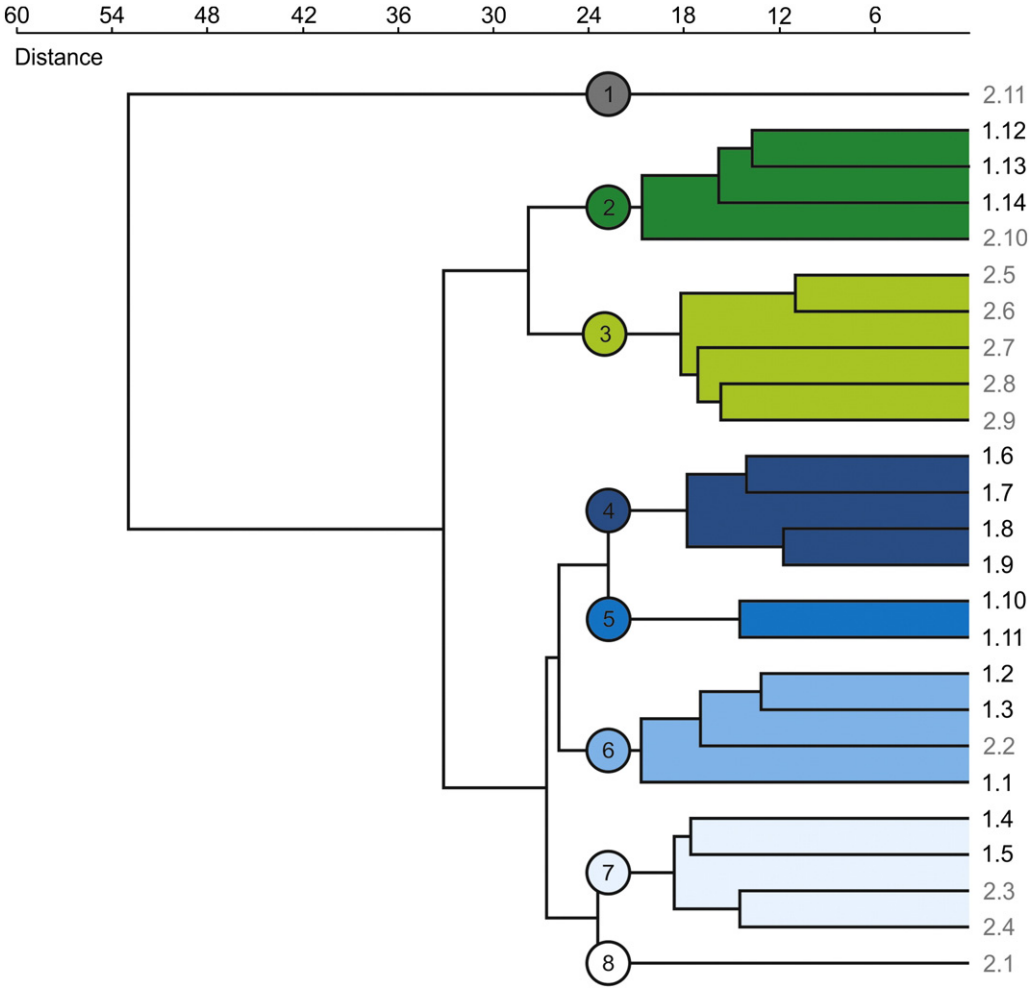

Fig. 5. Cluster analysis (Euclidean distance, paired-group; coph. corr.: 0.87) for benthic foraminiferal assemblages >125 μm (combined fractions) at IODP Site U1385. Circled numbers indicate groups of samples with a similar composition that represent distinct assemblages used for palaeoenvironmental interpretation. See Table 2 for taxa that determine clusters.

vanishes rapidly and disappears following the YD. Assemblages of MIS 1 are characterized by *Bulimina mexicana*, *B. alazanensis*, *Hoeglundina elegans* and *Gyroidinoides* spp. as most common foraminifers. Amongst the generally rare agglutinated shells, *Eggerella bradyi* is the only species that occurs regularly. Increased abundances of agglutinated shells between 0.20 and 0.80 m mcd are related to the presence of *Hyperammina* spp., *Rhizammina algaeformis* and *Saccorhiza ramosa*.

M. barleeanum, preferring an intermediate infaunal habitat, is restricted to rare occurrences in MIS 2 and HS 1. Deep infaunal taxa are almost exclusively represented by *Globobulimina* spp., *Chilostomella oolina* occurs rarely (Fig. 3; Supplementary Table 1). Values ≥10% occur during MIS 2 and across Termination I with peak values >30% during HS 1. Following the YD, deep infaunal taxa disappear rapidly.

4.1.2. 125–212 μm

Shells of the smaller size-fraction contribute 59–85% (A = 73%, σ = 7%) to the combined fractions with distinct peaks during MIS 1 and MIS 2, and trends resemble those of the combined fractions. Numbers of benthic foraminifera/g (12–40/g; A = 25/g, σ = 8/g) are highest during MIS 2 and decrease abruptly with the onset of HS 1. Hyaline shells (12–34/g; A = 20/g, σ = 8/g) are clearly dominant while miliolid (0–9/g; A = 3/g, σ = 3/g) and agglutinated shells (0–4/g; A = 1/g, = 1/g) are rare (Fig. 3; Supplementary Table 1).

Assemblages are dominated by hyaline foraminifera (69–96%; A = 82%, σ = 10%) with peak values during MIS 2, HS 1 and MIS 1. Conversely, miliolid shells (2–30%; A = 14%, σ = 11%) are most abundant across Termination I, mainly due to increased abundances of *Pyrgo* spp. and *Triloculina* spp. While changes in assemblage composition generally follow the pattern observed for the combined fractions, there are subtle differences in the abundances of certain taxa. E.g., *B. alazanensis*, *C. neoteretis* and *E. exigua* are more abundant, while *Globobulimina* spp., *H. elegans* and *Pyrgo* spp. are diminished (Fig. 4; Supplementary Table 2). Agglutinated foraminifera are generally rare with *E. bradyi* as the only regularly occurring species. Increased values in the upper part of the core are related to *Hyperammina* spp., *R. algaeformis*, *S. ramosa* and undetermined shell fragments.

The abundances of intermediate and deep infaunal taxa are diminished compared to the combined fractions, and almost exclusively represented by *Globobulimina* spp. (Fig. 3; Supplementary Table 1). Highest values ≥17% occur during HS 1, and they disappear with the inception of MIS 1.

4.1.3. >212 μm

Shells >212 μm contribute up to 41% to the combined assemblages (15–41%; A = 27%, σ = 7%) and have their highest abundances (≥30%) from the BAIS to the inception of MIS 1. Generally low numbers of benthic foraminifera/g (3–17/g; A = 9/g, σ = 4/g) show only minor fluctuations during MIS 2 and across Termination I, until a marked decrease occurs with the inception of MIS 1. Hyaline shells (2–13/g; A = 6/g, σ = 3/g) are primarily responsible for this trend, while

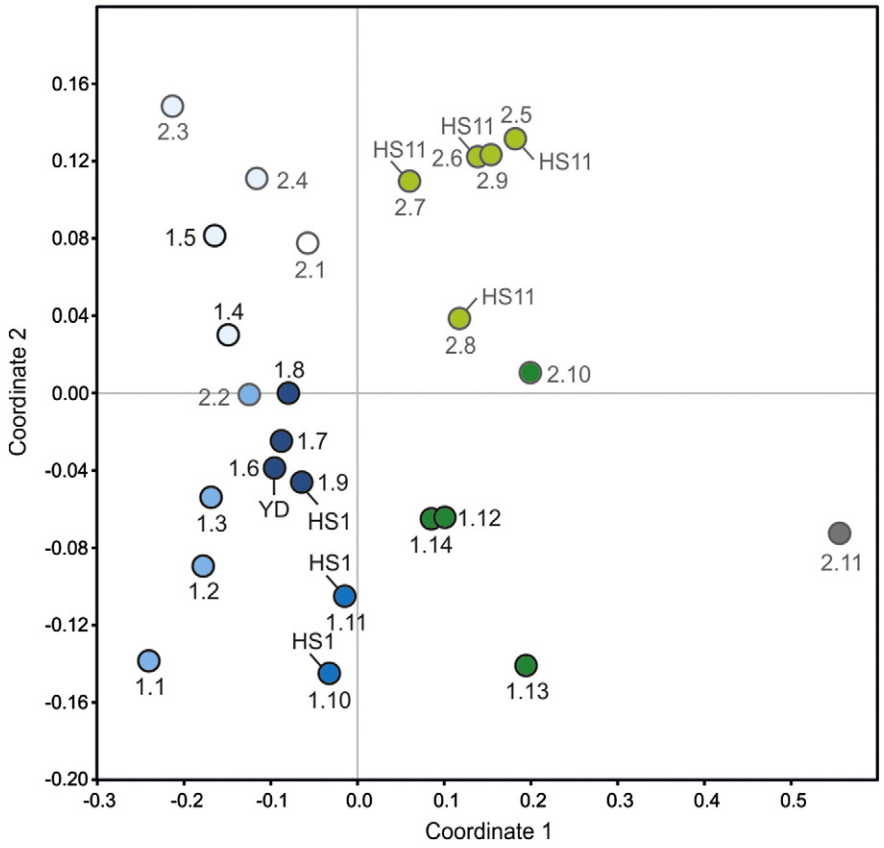

Fig. 6. Non-metric multidimensional scaling (nMDS) analysis (Euclidean distance; stress = 1.6) for benthic foraminiferal assemblages >125 μm (combined fractions) at IODP Site U1385. Colours refer to the assemblages identified in Fig. 5.

elevated numbers of miliolid shells (0–5/g; A = 2/g, σ = 1/g) are restricted to Termination I (Fig. 3; Supplementary Table 1). Agglutinated shells (0–1/g; A = 1/g, σ = 0/g) are almost absent throughout.

Similar to the smaller and combined fractions, assemblages are dominated by hyaline foraminifera (43–89%; A = 71%, σ = 13%) with peak values ≥ 78% during MIS 2 and HS 1. However, miliolid shells are comparably more abundant (3–55%; A = 22%, σ = 14%) with values up 55% from the BAIS to the inception of MIS 1. Generally, species richness of the assemblages > 212 μm is impoverished and characterized by the dominance of a few species resulting in a stronger contrast in abundances and more pronounced shifts in assemblage composition. During MIS 2 and HS 1, *Globobulimina* spp. dominate the assemblages with

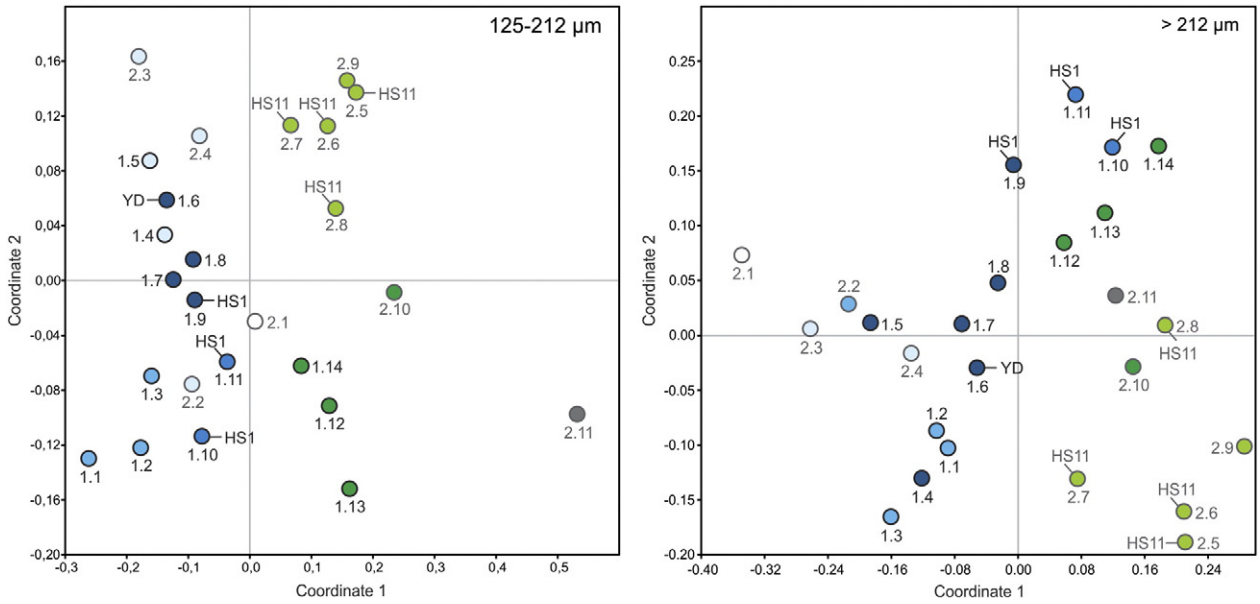

Fig. 7. NMDS analysis (Euclidean distance; stress = 1.5) for benthic foraminiferal assemblages 125–212 μm (left) and >212 μm (right) at IODP Site U1385. Colours refer to the assemblages identified in Fig. 5.

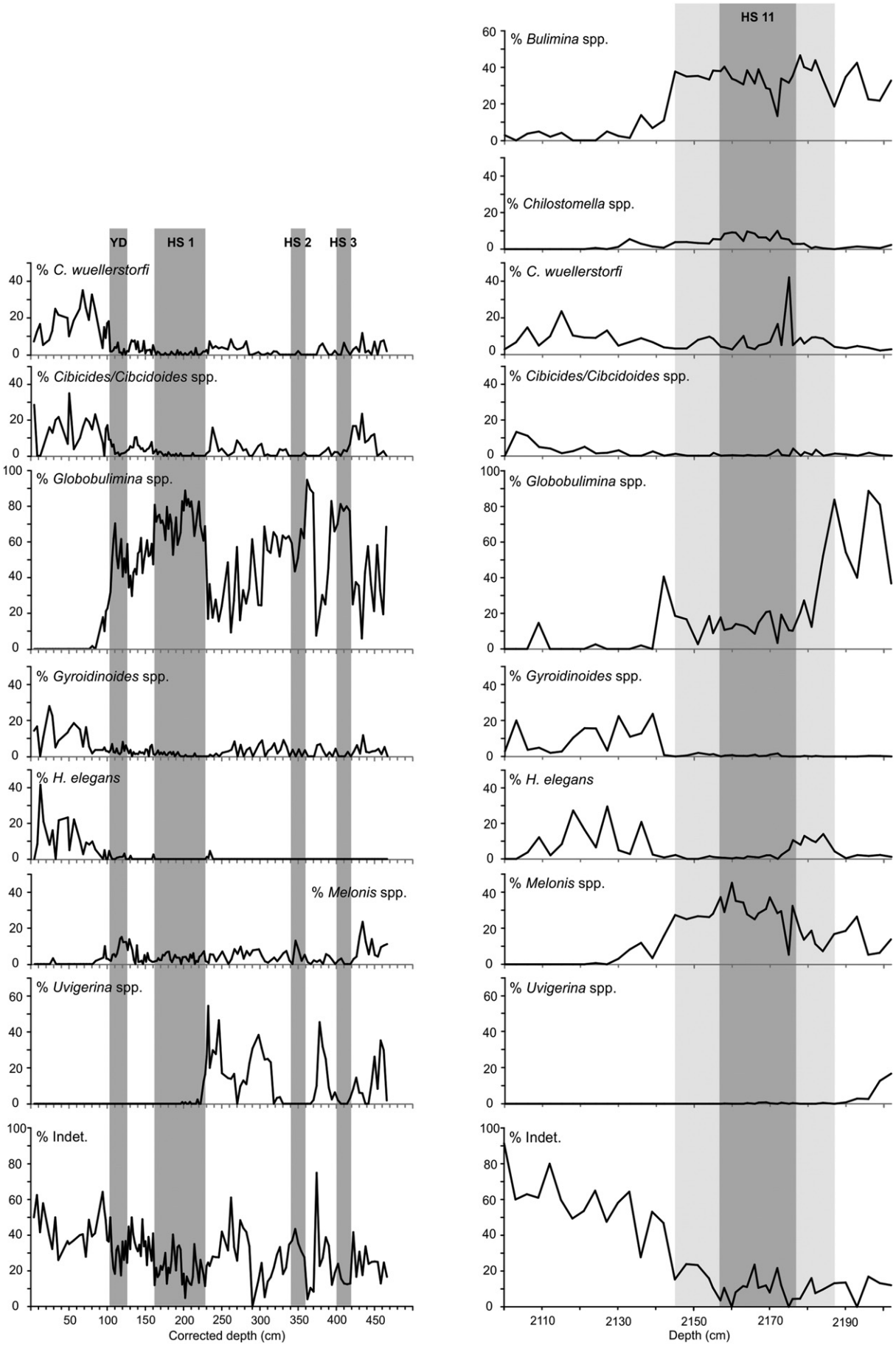
YD
HS 1
HS 2
HS 3
HS 11
% C. wuellerstorfi
% Cibicides/Cibcidoides spp.
% Globobulimina spp.
% Gyroidinoides spp.
% H. elegans
% Melonis spp.
% Uvigerina spp.
% Indet.
% Bulimina spp.
% Chilostomella spp.
Corrected depth (cm)
Depth (cm)

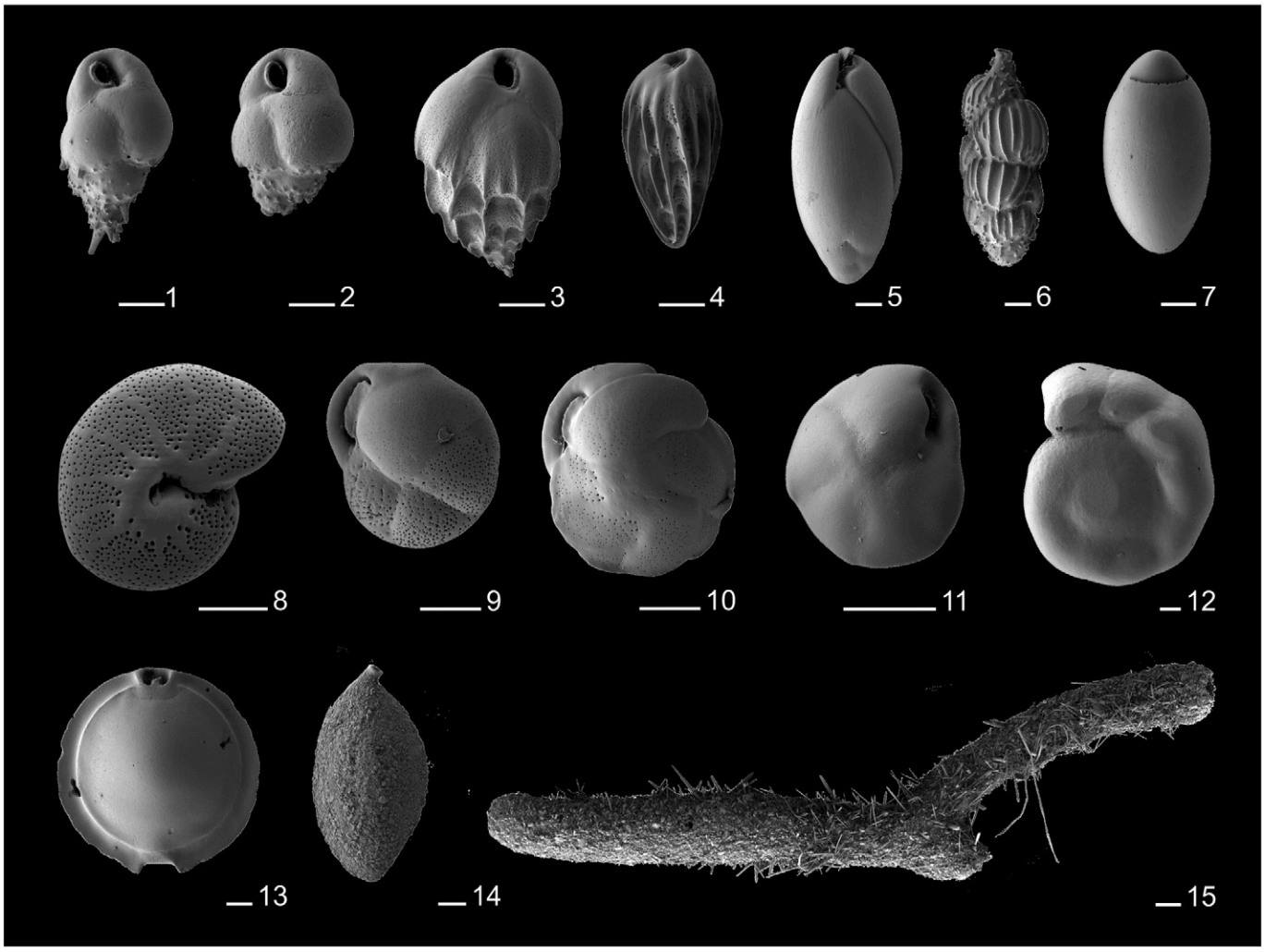

Plate 1. Common taxa of benthic foraminifera identified in the present study. For taxonomic notes see Appendix A. Scale bar next to reference number corresponds to 100 μm.

1. *Bulimina aculeata* d'Orbigny, 1826. U1385E-3H-6W-40-41.
2. *Bulimina marginata* d'Orbigny, 1826.U1385E-6H-1W-120-121.
3. *Bulimina mexicana* d'Orbigny, in Guérin-Méneville, 1843. U1385E-6H-2W-80-81.
4. *Bulimina alazanensis* Gümbel, 1868. U1385D-1H-3W-20-21.
5. *Globobulimina affinis* (d'Orbigny, 1839). U1385D-1H-3W-20-21.
6. *Uvigerina pigmea* d'Orbigny, 1826. U1385E-6H-2W-0-1.
7. *Chilostomella oolina* Schwager, 1878. U1385E-3H-5W-140-141.
8. *Melonis barleeanum* (Williamson, 1858). U1385E-3H-5W-140-141.
9. *Globocassidulina minuta* (Cushman, 1933). U1385E-3H-6W-80-81.
10. *Cassidulina neoteretis* Seidenkrantz, 1995. U1385E-3H-6W-80-81.
11. *Epistominella exigua* (Brady, 1884). U1385E-3H-5W-100-101.
12. *Gyroidinoides soldanii* (d'Orbigny, 1826). U1385E-3H-5W-100-101.
13. *Pyrgo murrhina* (Schwager, 1866). U1385E-3H-5W-80-81.
14. *Sigmoilopsis schlumbergeri* (Silvestri, 1904). U1385D-1H-2W-80-81.
15. *Saccorhiza ramosa* (Brady, 1879). U3185D-1H-1W-0-1.

abundances up to 48%, accompanied by minor abundances of *B. alazanensis*, *C. neoteretis* (MIS 2), *M. barleeanum* (MIS 2) and *M. pompilioides* (HS 1). This assemblage deteriorates during the BAIS and the inception of MIS 1 with a parallel increase in *B. mexicana* and miliolid taxa (fragments, many of them cf. *Pyrgo*, together with *Pyrgo* spp. and *S. schlumbergeri*). After a short-lived bloom during the YD, *Globobulimina* spp. and *Melonis* spp. finally disappear. Assemblages of *Cibicidoides* spp. (mainly *Cibicidoides wuellerstorfi*), *B. mexicana*, *Gyroidinoides* spp. (mainly *G. soldanii*) and *H. elegans* characterize MIS 1 (Fig. 4; Supplementary Table 2). Agglutinated foraminifera are a minor component except for the interval between 0.20 and 0.80 m mcd in which fragments of *Hyperammina* spp., *R. algaeformis*,

Fig. 8. Abundances of benthic foraminiferal taxon groups at MD99-2334 K (left) and MD01-2444 (right). Positions of the Younger Dryas and Heinrich stadials 1, 2, 3, and 11 have been adopted from Skinner et al. (2003), Skinner and Shackleton (2006) and Hodell et al. (2013a). Light grey area indicates extension of IRD deposition related to HS 11 (Skinner and Shackleton, 2006).

S. ramosa and others show increased abundances. *E. bradyi* is the most abundant agglutinated foraminifer showing increased values (9%) during MIS 2.

The abundances of intermediate and deep infaunal taxa mainly follow the abundances of *Globobulimina* spp. and vary widely between 0% and 55% (Fig. 3; Supplementary Table 1). Values ≥ 20% occur during MIS 2 and across Termination I, and they are absent following the YD.

4.2. U1385E-3H — low resolution record of Termination II

4.2.1. >125 μm

For most samples, numbers of benthic foraminifera/g (17–126/g; A = 64/g, σ = 35/g) are considerably higher compared to Termination I. A stepwise decrease occurs across Termination II with highest values during MIS 6 and late HS 11, and abrupt decreases at the onset and end of HS 11. While hyaline shells (12–122/g; A = 57/g, σ = 37/g) determine trends during MIS 6 and HS 11, miliolid shells (2–21/g; A = 6/g, σ = 6/g) contribute considerably during MIS 5e (Fig. 3; Supplementary Table 1). Agglutinated shells (0–2/g; A = 1/g, σ = 1/g) are almost absent.

Samples are generally dominated by hyaline foraminifera (57–97%; A = 84%, σ = 16%) with peak values during MIS 6 and HS 11, miliolid foraminifera (2–40%; A = 14%, σ = 14%) show considerably increased values after HS 11. Similar to the U1385D-1H data-set, faunal changes occur across Termination II but the composition is different. MIS 6 and HS 11 are characterized by often antagonistic fluctuations of *C. neoteretis*, *Bulimina marginata*, *Uvigerina pigmea*, *Melonis* spp., *Globobulimina* spp. and *Bulimina aculeata*. Most notably, the onset of HS 11 is marked by an abrupt decrease in *Globobulimina* spp. and increases in *M. pompilioides*. *M. barleeanum* shows highest values in the late HS 11. These taxa quickly diminish with the end of HS 11 and are replaced by *B. alazanensis*, *E. exigua*, *Gyroidinoides* spp. and miliolid taxa (fragments, many of them cf. *Pyrgo*, and *Pyrgo* spp. (Fig. 4, Supplementary Table 2)). *E. bradyi* is the only agglutinated foraminifer that occurs regularly throughout the samples. Tube-shaped shells of *Hyperammina* spp., *R. algaeformis* and *S. ramosa* are absent from the samples.

In contrast to Termination I, the intermediate infaunal *M. barleeanum* is abundant during MIS 6 and HS 11 while deep infaunal taxa, mainly represented by *Globobulimina* spp., are less abundant. Deep infaunal taxa are most abundant (up to 16%) during MIS 6, *M. barleeanum* in late HS 11.

4.2.2. 125–212 μm

Shells of the smaller size-fraction contribute slightly larger portion (70–85%; A = 77%, σ = 5%) to the combined data-sets compared to U1385D-1H, and similarly trends of the smaller fraction largely resemble those of the combined fractions. Numbers of benthic foraminifera/g (13–108/g; A = 49/g, σ = 29/g) show an overall decrease with highest values during MIS 6 and late HS 11. Hyaline shells (11–105/g; A = 45/g, σ = 30/g) generally determine this trend except for the interval following HS 11 (21.62–21.82 m mcd) in which miliolid shells (1–13/g; A = 4/g, σ = 4/g) increase (Fig. 3; Supplementary Table 1). Agglutinated shells are almost absent throughout.

Changes in the assemblages are reflected in antagonistic fluctuations in the abundances of the generally dominant hyaline shells (63–98%; A = 87%, σ = 13%) and the less abundant miliolid shells (2–33%; A = 12%, σ = 12%). The latter show a considerable increase following HS 11, mainly due to fragments (many of them cf. *Pyrgo*) and *Pyrgo* spp. Similar to U1385D-1H, changes in assemblage composition follow the pattern observed for the combined fractions with subtle differences in the abundances of certain taxa compared to the combined fractions. E.g., *C. neoteretis* and *E. exigua* are more abundant, while *Globobulimina* spp., *H. elegans*, *U. pigmea* and *Pyrgo* spp. are diminished (Fig. 4; Supplementary Table 2). Other taxa, notably *Globocassidulina minuta* (MIS 6), *Gc.* cf. *rossensis* (MIS 5e) and *Nuttallides umbonifera* (MIS 5e), show increased abundances in individual samples compared to the other size-fractions.

The abundances of intermediate and deep infaunal taxa follow the same trends as in the combined fractions with slightly lower values (Fig. 3; Supplementary Table 1).

4.2.3. >212 μm

Shells of the larger size-fraction contribute 15–30% (A = 23%, σ = 5%) to the combined fractions, and similar to Termination I this size-fraction shows some differences to the smaller and combined fractions. Except for a peak prior to HS 11, numbers of benthic foraminifera/g (3–30/g; A = 14/g; σ = 7/g) show only minor fluctuations until a sudden decrease at the top of the core (21.22 m mcd). Trends are almost exclusively determined by hyaline shells (1–28/g; A = 12/g; σ = 8/g). Miliolid shells (0–5/g; A = 2/g; σ = 1/g) are of minor importance, agglutinated shells (0–1/g; A = 0.3/g; σ = 0.1/g) are almost absent (Fig. 3; Supplementary Table 1).

In contrast to the smaller and combined fractions, the dominance of hyaline foraminifera (28–96%; A = 73%, σ = 26%) is restricted to MIS 6 and HS 11. With the end of HS 11, miliolid shells (3–63%; A = 24%, σ = 24%) begin to dominate. Similar to U1385D-1H, assemblages >212 μm are comparably impoverished in their faunal inventory (most notably, *C. neoteretis* is almost completely absent), and fewer species determine more pronounced shifts in composition. During MIS 6, *B. aculeata*, *B. marginata* and *Globobulimina* spp. are consistently abundant together with occasional increases in *U. pigmea* and *M. pompilioides*. With the onset of HS 11, a sudden decrease in *Globobulimina* spp. is paralleled by an increase in *M. pompilioides*. The later phase of HS 11 shows highest abundance of *M. barleeanum* and *Cibicidoides* spp. (mainly *C. wuellerstorfi*). *B. aculeata* and *B. marginata* stay abundant throughout HS 11. With the end of the termination, miliolid shells (fragments, many of them cf. *Pyrgo*, and *Pyrgo* spp.) become dominant and no hyaline species show increased abundances except for individual samples (*C. bradyi*, *C. wuellerstorfi*, *Osangularia culter*; Fig. 4; Supplementary Table 2). Agglutinated foraminifera (1–10%; A = 4%, σ = 3%) are generally rare except for the top (21.02–21.22 m mcd) where *E. bradyi* and other Eggerellinae show slightly increased abundances.

Abundances of intermediate and deep infaunal taxa are more pronounced than in the combined and smaller fractions but generally follow the same pattern with high abundances during MIS 6 and HS 11, and absence during MIS 5e (Fig. 3; Supplementary Table 1).

4.3. Multivariate statistical analysis of the low-resolution data-sets

4.3.1. >125 μm

Eight distinct groups of samples are differentiated in the cluster and nMDS analyses based on their dissimilarity (Figs. 5, 6). SIMPER analysis reveals that the grouping is caused by a small number of taxa: *C. neoteretis* and miliolids contribute ~45% to the dissimilarity between the identified groups, *B. marginata*, *E. exigua*, *B. mexicana*, *B. alazanensis*, *Pyrgo* spp., and *Gyroidinoides* spp. contribute another ~30% (Table 2; Supplementary Table 3). Assemblages 1–3 occur during glacial stages MIS 2 and 6 and HS 11, assemblages 4 and 5 contain samples of HS 1, the BAIS, and the YD, and assemblages 6–8 are associated with interglacial stages MIS 1 and MIS 5e (Fig. 5). In the nMDS analysis, assemblages 1–3 and 4–8 are well separated along coordinate 1, indicating parallel trends in both data-sets. In contrast, coordinate 2 is characterized by a distinct offset between of the data-sets of Terminations I and II (Fig. 6).

4.3.2. 125–212 μm

NMDS analysis reveals results similar to the combined fractions >125 μm (Fig. 7). SIMPER analysis shows that the grouping is largely determined by the same taxa: *C. neoteretis* and *B. marginata* contribute ~50% to the dissimilarity between the identified groups, miliolids, *E. exigua*, *B. alazanensis* and *B. mexicana* contribute another ~28% (Supplementary Table 3). The same groups of samples as in the

Table 1
Abundances of benthic foraminiferal shell types and key-taxa in mudline samples of IODP Sites U1385B, C, and E compared to samples 1.1–1.3 of the MIS 1 interval at IODP Site U1385D (see Fig. 2). For the mudlines samples, relative abundances have been calculated for total and reduced (i.e., exclusion of astrorhizoid taxa) assemblages. See text for details. Bold numbers indicate taxa that show abundances >5%.

	U1385B		U1385C		U1385E		Total		Reduced		MIS 1	
	Total	Reduced	Total	Reduced	Total	Reduced	Mean	Stdv	Mean	Stdv	Mean	Stdv.
Hyaline	**22.4**	**68.7**	**12.7**	**71.7**	**16.8**	**69.6**	**17.3**	4.9	**70.0**	1.6	**81.0**	5.3
Miliolid	2.8	**8.7**	0.8	4.3	3.7	**15.2**	2.4	1.5	**9.4**	5.5	**9.7**	3.6
Agglutinated	**74.1**	**22.6**	**86.5**	**23.9**	**79.6**	**15.2**	**80.1**	6.2	**20.6**	4.7	**9.3**	6.1
Astrorhizoid taxa	**63.4**	–	**78.8**	–	**73.3**	–	**71.8**	7.8	–	–	2.4	2.2
Triloculina spp.	0.3	0.9	0.0	0.0	1.6	**6.5**	0.6	0.8	2.5	3.5	0.0	0.0
Bolivinids	2.6	**7.8**	0.0	0.0	2.5	**10.9**	1.7	1.5	**6.2**	5.6	1.1	0.9
B. alazanensis	3.7	**11.3**	1.5	**8.7**	1.0	4.3	2.1	1.4	**8.1**	3.5	**12.4**	2.0
B. mexicana	0.3	0.9	0.0	0.0	0.0	0.0	0.1	0.2	0.3	0.5	**12.5**	6.2
C. oolina	2.6	**7.8**	0.0	0.0	0.5	2.2	1.0	1.4	3.3	4.0	0.0	0.0
Cibicids	0.0	0.0	1.2	**6.5**	1.0	4.3	0.7	0.6	3.6	3.3	3.8	0.4
E. exigua	0.6	1.7	0.8	4.3	0.5	2.2	0.6	0.1	2.8	1.4	**7.9**	5.1
Fissurina spp.	1.7	**5.2**	1.5	**8.7**	2.1	**8.7**	1.8	0.3	**7.5**	2.0	1.3	1.2
Gyroidinoides spp.	1.1	3.5	3.1	**17.4**	1.6	**6.5**	1.9	1.0	**9.1**	7.3	**12.7**	0.6
H. elegans	0.0	0.0	0.8	4.3	0.5	2.2	0.4	0.4	2.2	2.2	3.7	1.4
O. umbonatus	0.0	0.0	0.0	0.0	0.5	2.2	0.2	0.3	0.7	1.3	3.3	2.2
T. rhomboidalis	0.0	0.0	0.0	0.0	0.0	0.0	0.0	0.0	0.0	0.0	4.6	2.4

combined fractions are separated along coordinate 1 of the nMDS analysis although samples of HS 1 show greater similarities with MIS 2. The differentiation between samples of Terminations I and II along coordinate 2 is not as well expressed, in particular during interglacial periods MIS 2 and MIS 6 (Fig. 7).

4.3.3. >212 μm

NMDS analysis reveals some remarkable differences compared to the smaller and combined fractions (Fig. 7). SIMPER analysis indicates that the grouping is caused by a group of taxa different from fractions >125 μm and 125–212 μm: *Pyrgo* spp., *Globobulimina affinis, B. aculeata* and miliolids contribute ~50% to the dissimilarity, *Globobulimina* sp.1, *H. elegans*, *M. barleeanum* and *C. neoteretis* another ~25% (Supplementary Table 3). While samples of MIS 1, MIS 5e and the YD are still well separated from those of MIS 2, MIS 6 and HS 11 along coordinate 1, the assemblages of HS 1 shows greater similarities with the latter. Similar to 125–212 μm, the differentiation between samples of Terminations I and II along coordinate 2 is not as well expressed (Fig. 7).

4.4. MD99-2334 K — high resolution record of Termination I

Assemblages at this site are determined by a few taxa which, on average, represent 71% ($\sigma = 13\%$) of all benthic foraminifera: *Cibicidoides* spp., *Globobulimina* spp., *Gyroidinoides* spp., *H. elegans*, *Melonis* spp., and *Uvigerina* spp. (Fig. 8; Supplementary Table 4). Highest numbers of indeterminate taxa are associated with interstadial periods and MIS 1, during the later related to a marked increase in miliolid shells. A distinct faunal turnover is associated with Termination I: MIS 2 and HS 1–3 are characterized by antagonistic fluctuations in *Globobulimina* spp. and *Uvigerina* spp., the latter being abundant in interstadial periods and absent in HS 1–3. *Globobulimina* spp. remains dominant across Termination I, until it disappears rapidly with the end of the YD. Parallel

Table 2
SIMPER analysis (Euclidean distance) for benthic foraminifera >125 μm (combined fractions), highlighting taxa determining assemblages 1–8 (Fig. 5). Species that show abundances <5% in the assemblages have been summarized in their respective genera. Bold numbers indicate taxa that show an abundance of >4% in their respective assemblage.

Taxon	Average dissimilarity	Contribution (%)	Cumulative %	Ass. 1	Ass. 2	Ass. 3	Ass. 4	Ass. 5	Ass. 6	Ass. 7	Ass. 8
Samples in assemblage				2.11	1.12–1.14; 2.10	2.5–2.9	1.6–1.9	1.10–1.11	1.1–1.3; 2.2	1.4–1.5; 2.3–2.4	2.1
Cassidulina neoteretis	377.40	33.81	33.81	**55.0**	**23.5**	**12.6**	0.5	2.5	0.8	1.3	**14.0**
Miliolidae indet.	127.00	11.38	45.19	2.0	1.5	3.4	**6.5**	0.0	**5.3**	**21.5**	**13.0**
Bulimina marginata	122.70	10.99	56.18	3.0	2.3	**17.8**	0.0	0.0	0.0	1.0	0.0
Epistominella exigua	60.61	5.43	61.61	1.0	**13.8**	**5.2**	**8.0**	**4.5**	**9.5**	**6.0**	**13.0**
Bulimina alazanensis	50.82	4.55	66.16	0.0	1.3	0.0	0.3	**8.5**	**11.8**	3.0	**8.0**
Bulimina mexicana	49.73	4.46	70.62	0.0	1.0	0.6	**7.3**	1.5	**9.5**	3.5	1.0
Pyrgo spp.	33.55	3.01	73.63	1.0	0.8	1.6	**7.0**	0.5	**4.3**	**8.5**	**12.0**
Gyroidinoides spp.	30.69	2.75	76.37	0.0	2.3	0.6	3.3	3.0	**11.3**	**4.3**	**5.0**
Globobulimina affinis	28.30	2.54	78.91	3.0	**4.8**	3.4	**4.3**	**12.5**	0.0	2.0	0.0
Melonis barleeanum	24.97	2.24	81.15	1.0	2.0	**6.4**	0.0	0.5	0.0	0.8	0.0
Bulimina aculeata	20.83	1.87	83.01	2.0	1.0	**7.4**	0.0	0.0	0.0	0.8	0.0
Melonis pompilioides	20.71	1.86	84.87	1.0	1.8	**4.8**	**5.3**	**5.0**	0.0	2.3	0.0
Globobulimina sp.1	20.66	1.85	86.72	1.0	2.3	1.0	**6.3**	**7.5**	0.0	0.8	0.0
Triloculina sp.1 (*T. elongotricarinata*?)	11.12	1.00	87.71	0.0	2.5	0.0	**4.0**	0.5	0.0	1.8	0.0
Hoeglundina elegans	10.97	0.98	88.7	0.0	0.0	0.8	3.3	0.5	2.8	3.3	0.0
Globobulimina spp.	10.60	0.95	89.65	3.0	**4.8**	2.6	2.5	**5.5**	0.0	1.5	0.0
Globocassidulina minuta	10.59	0.95	90.6	**9.0**	2.0	1.4	0.0	0.5	0.3	0.0	0.0
Sigmoilopsis schlumbergeri	7.54	0.68	91.27	0.0	1.3	0.2	**4.8**	1.5	1.8	1.8	1.0
Pullenia spp.	7.01	0.63	91.9	2.0	3.8	1.6	3.5	**5.5**	2.5	2.3	1.0
Tortoplectella rhomboidalis	6.39	0.57	92.47	0.0	0.3	0.8	0.0	0.0	4.3	1.0	2.0
Sphaeroidina bulloides	6.13	0.55	93.02	0.0	1.0	0.0	1.5	5.5	0.0	0.5	1.0
Agglutinated indet.	5.78	0.52	93.54	0.0	0.0	0.2	0.0	0.0	2.8	0.0	0.0
Nuttallides umbonifera	5.57	0.50	94.04	0.0	0.3	0.8	0.3	0.0	0.3	1.8	**7.0**
Hyaline indet.	4.75	0.43	94.46	3.0	**4.8**	**5.6**	3.5	**5.0**	3.0	3.8	1.0

increases in the abundances of *Cibicidoides* spp., *Gyroidinoides* spp. and *H. elegans* characterize MIS 1.

4.5. MD01-2444 — high resolution record of Termination II

In addition to the key-taxa identified at MD99-2334 K, *Bulimina* spp. and *Chilostomella* spp. constitute important elements of this data-set (Fig. 8; Supplementary Table 5). On average, the determined taxa represent 73% ($\sigma = 25\%$) of the assemblage. Similar to MIS 2, *Globobulimina* spp. is the dominant taxon during glacial conditions prior to HS 11, showing inverse fluctuations to *Bulimina* spp. and *Melonis* spp. while *Uvigerina* spp. is generally rare. While increased abundances of *Bulimina* spp. persist during HS 11, a marked decrease in *Globobulimina* spp. occurs at its onset paralleled by increases in *Melonis* spp. and *Chilostomella* spp. With the end of HS 11 and the onset of MIS 5e, abundances of these taxa deteriorate rapidly, giving rise to *Cibicidoides* spp., *Gyroidinoides* spp. and *H. elegans*, similar to MIS 1. However, in contrast to MD99-2334 K, indeterminate taxa increase rapidly up to 91% after HS 11, mainly related to a considerable increase in miliolid shells.

4.6. Mudline samples

Mudline samples contain an average 80% agglutinated, 17% hyaline, and 3% miliolid shells (Table 1). Minor variations in assemblage composition occur between the three sites, but overall they are very similar. Tubular astrorhizoid shells represent the most abundant group of agglutinated taxa. No hyaline taxa show abundance of more than 5% at any site, bolivinids, buliminids (in particular *B. alazanenis*), *Fissurina* spp. and *Gyroidinoides* spp. are most common.

5. Discussion

5.1. Taphonomic bias on benthic foraminiferal assemblages of the southwestern Iberian Margin

Present-day assemblages of benthic foraminifera in the study area contain high proportions of foraminifera with agglutinated shells, particularly at sites bathed in NEADW and LDW where these foraminifera amount to 70–90% (Phipps et al., 2012). This pattern also characterizes the mudline assemblages from IODP Sites U1385B, U1385C, and U1385E which contain on average ~80% of agglutinated shells (Table 1). A severe decrease in the abundance of agglutinated shells apparently occurs within the first 20 cm below the mudline, and their contribution to the fossil assemblages never exceeds 16% and remains <5% in most of the samples studied. A similar decline within the first 10–20 cm of deep-sea sediments has been reported from other sites and attributed to selective preservation of hard-shelled carbonate over soft-shelled agglutinated foraminiferal shells (Schröder, 1988; Kuhnt et al., 2000; Schröder-Adams and van Rooyen, 2011; Lejzerowicz et al., 2013). Strong indications that the decline of agglutinated shells at U1385 is a taphonomic rather than a biological signal arise from two observations. First, most agglutinated shells in the mudline samples represent tube-shaped, furcate and non-furcate, uni- and bilocular morphotypes of astrorhizoid taxa. These foraminifers build their shells from sedimentary particles embedded in a proteinaceous or mineralized matrix (= soft shells in Schröder, 1988) and occupy epifaunal and shallow infaunal microhabitats (Kuhnt et al., 2000). Both factors make the shells especially prone to post-mortem disintegration by bacterial decay and/or transportation (Goldstein and Barker, 1988; Schröder, 1988; Kuhnt et al., 2000). In the fossil assemblages, following the severe reduction of agglutinated shells to ≤16%, soft-shelled foraminifera are present to a small extent as fragments of *Hyperammina*, *Rhabdammina*, *Rhizammina* and *Saccorhiza* down to 80 cm below the sediment surface. Below this level, fragments of these taxa vanish, and agglutinated shells remain ≤8% for the U1385D data-set and ≤5% for the U1385E data-set. This residual agglutinated fauna consists of firmly cemented tests of infaunal taxa such as *Eggerella* and *Karreriella* that have a comparably high fossilization potential (Schröder, 1988; Kuhnt et al., 2000).

Second, if astrorhizoid shells are excluded from the mudline samples, the ratio of agglutinated to miliolid to hyaline shells (21%/9%/70%) as well as the composition (*B. alazanensis* and *Gyroidinoides* spp. as most abundant taxa) of the residual mudline assemblages resembles that of samples 1.1–1.3 from MIS 1 (Table 1). Minor differences in composition are most likely explained by patchy distribution (apparent in the faunal variability between mudline samples; Gooday and Rathburn, 1999; Griveaud et al., 2010) as well as the partial loss of foraminifera during the mudline sampling process. It is thus reasonable to assume that astrorhizoid foraminifera have been the dominant component of the fossil assemblages at least during MIS 1, i.e. the taphocoenoses of this interval most likely represent not more than ~30% of the original assemblages. For the time preceding MIS 1, it is not possible to give an estimate on the loss of agglutinated shells as export productivity and water-mass distribution, and thus environmental conditions at the sea-floor, differed from today (Voelker and de Abreu, 2011). However, present-day assemblages contain >70% of agglutinated shells at sites bathed by NEADW and up to 90% in LDW, two water masses that differ significantly in their nutrient and oxygen content (Phipps et al., 2012). As glacial/interglacial and stadial/interstadial changes in the study area are characterized by fluctuations in the depth of the NEADW/LDW interface (Skinner et al., 2003; Voelker and de Abreu, 2011), it seems reasonable to assume that agglutinated shells have originally been the major component in the order of >70% of all studied samples regardless of the climate state (the composition of the agglutinated assemblages, however, might have differed; Phipps et al., 2012). Assuming no major variations occurred in the total abundance of agglutinated shells between glacial and interglacial conditions, differences in the composition of the fossil assemblages as revealed by multivariate statistical analysis still carry qualitative palaeoenvironmental information. However, the relative proportions of taxa are clearly overstated, and changes in the abundances of those benthic foraminifera revealed most significant by SIMPER analysis are useful as index taxa.

Another aspect concerns the application of the TROX concept to the assemblages (Jorissen et al., 1995, 2007; Jorissen, 2003). This well-tested concept links the microhabitat of benthic foraminiferal species to two contrasting environmental parameters, food availability and oxygenation: Epifaunal taxa dominate oligotrophic, well ventilated environments, whereas deep infaunal taxa are more abundant in eutrophic, poorly oxygenated environments (Jorissen et al., 2007). Between these end-members, a more equal distribution of epi- and infaunal microhabitats occurs in intermediate, mesotrophic environments. The loss of large portions of epifaunal and shallow infaunal taxa at U1385 would thus result in the overestimation of trophic conditions and/or underestimation of oxic conditions if the TROX concept is applied in a straightforward manner. This bias is evident in the mudline assemblages: if astrorhizoid shells are excluded, the well diversified distribution of epifaunal, shallow, intermediate and deep infaunal microhabitats would imply a mesotrophic to eutrophic sea-floor environment (Jorissen et al., 2007; Phipps et al., 2012). When including the complete agglutinated fauna, epifaunal and shallow infaunal taxa are clearly dominant, and the indicated oligotrophic to slightly mesotrophic sea-floor environment describes present-day conditions very well (Phipps et al., 2012). This strong bias is considered in the present study by a cautious and limited application of the TROX concept. First, the combined abundances of intermediate (*M. barleeanum*) and deep infaunal (*Chilostomella* spp., *Globobulimina* spp.) taxa, reflecting a well-tiered microhabitat distribution, are applied as indicators of mesotrophic conditions with intermediate ventilation (Jorissen, 2003). Second, we apply the abundances of deep infaunal taxa adapted to low oxic conditions (*Chilostomella* spp., *Globobulimina* spp.) as a qualitative proxy for extremely depressed oxygenation levels (Jorissen et al., 2007). Finally, another indication of deteriorated trophic conditions and improved

oxygenation is provided by the ratio of miliolid to hyaline shells. *Pyrgo*, which is the most abundant miliolid taxon at U1385, is indicative of comparably well-ventilated, oligotrophic conditions (Kaiho, 1999).

As the benthic microhabitat is defined by both, oxygen and food availability, a modified approach based on the BFAR method of Herguera and Berger (1991) is introduced to estimate export productivity. The BFAR concept relies on the assumption that the total number of benthic foraminifera per gram in a given sample carries a quantitative signal of export productivity. Because of the loss of large portions of the original assemblages, the BFAR proxy is not applicable in its original form at U1385. However, we argue that the number of benthic foraminifera with hyaline (perforate) shells per gram can be used for an assessment of qualitative changes in export productivity. The agglutinated/carbonate shell ratio in the study area is largely determined by export productivity (Phipps et al., 2012), and higher trophic demands of hyaline foraminifera result in an increase of their standing stock with increasing food availability. The number of hyaline foraminifera per gram sediment in the residual assemblages of U1385 thus indirectly reflects relative changes in trophic conditions (sedimentation rates are fairly constant at the studied sites, see Hodell et al., 2013b). We thus introduce the *hyaline* benthic foraminifera accumulation rate (hBFAR) as a qualitative proxy of export productivity for the present study (its application outside the study area remains to be tested).

In summary, a strong taphonomic bias on the composition of the fossil assemblages of the western Iberian Margin is evident, but they still retain a qualitative palaeoenvironmental signal if carefully interpreted. The considerations also suggest that studies relying on well-chosen and abundant taxa will yield reliable results (Caralp, 1987; Schönfeld et al., 2003). Proxy methods that require knowledge of the complete faunal inventory (e.g., TROX, BFOI, BFAR; Baas et al., 1998) have to be applied very cautiously and adapted to the taphonomic bias.

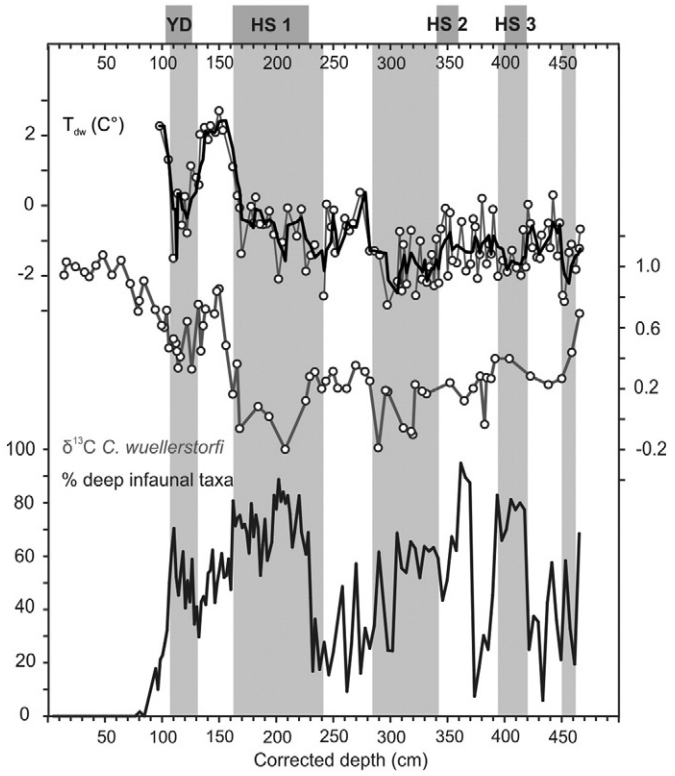

Fig. 9. Correlation of the abundance of deep-infaunal taxa (used as proxy of oxygen depletion) with existing geochemical records for deep-water temperature (T_{dw}; calculated from Mg/Ca values of *G. affinis*; Skinner et al., 2003; Skinner and Shackleton, 2006) and benthic δ^{13}C (*C. wuellerstorfi*; Skinner and Shackleton, 2004, 2006) for MD99-2334 K. Light grey areas indicate intervals of low T_{dw}.

5.2. Long-term trends in assemblages >125 μm across Terminations I and II

Multivariate statistical analyses of the benthic assemblages >125 μm indicate similarities as well as differences in the evolution of deep water hydrography across Terminations I and II. The separation of assemblages of MIS 2, MIS 6 and HS 11 from those of MIS 1, MIS 5e, HS 1 and the YD in the cluster analysis and along nMDS coordinate 1 reflects parallel trends from glacial to interglacial conditions in both data-sets (Figs. 5, 6). The separation is primarily determined by the abundances of *C. neoteretis* which is a frequent, sometimes dominant faunal element in MIS 2, MIS 6 and HS 11, but rare to absent in MIS 1, MIS 5e, HS 1 and YD samples. Today, *C. neoteretis* is restricted to the Arctic and boreal regions of the northern North Atlantic >46°N where it inhabits fine-grained, organic matter rich sediments of the continental shelf and slope down to 3000 m (Mackensen et al., 1985; Mackensen and Hald, 1988; Seidenkrantz, 1995). Bottom-water temperature seems to be a prime factor in its distribution as *C. neoteretis* commonly occurs at temperatures < 2 °C. The data indicate that this temperature threshold is crossed during both terminations which is supported by estimates of deep water temperature (T_{dw}) from Mg/Ca: present-day T_{dw} at IODP Site U1385 is ~3–3.5 °C, while T_{dw} has been estimated to be ~3–5 °C lower during MIS 2 and associated stadials, and ~1–3 °C during MIS 6 and HS 11 (Figs. 10, 11; Skinner et al., 2003; Skinner and Shackleton, 2006; Expedition 339 Scientists, 2013). The timing of the decrease in *C. neoteretis* differs between the terminations (Fig. 4): while it occurs rather abruptly with the onset of HS 1 despite prevailing cold T_{dw} (Fig. 9; Skinner et al., 2003), the species vanishes in two pulses over a longer time interval across HS 11. However, given the particularly high abundances of deep infaunal species in the HS 1 interval, the sudden decrease in *C. neoteretis* with the onset of this stadial might rather be related to poor oxygenation than warming T_{dw}. Although *Cassidulina teretis* s.l. has been occasionally reported from environments with oxygen concentrations as low as 0.5 ml/l, *Globobulimina* spp. and *Chilostomella* spp. are adapted to thrive in dysoxic and anoxic environments (Jorissen et al., 2007; Piña-Ochoa et al., 2010).

Export productivity is most likely a secondary component that contributes to the separation along coordinate 1. Besides *C. neoteretis* which thrives in organic rich sediments, the frequent occurrences of *Bulimina aculeata*, *B. marginata*, *Globobulimina* spp., *Melonis* spp., and *Uvigerina* spp. as well as elevated hBFAR values indicate increased organic matter flux to the sea floor during MIS 2, MIS 6, HS 11 and HS 1 (Altenbach et al., 1999; Jorissen, 1999; Morigi et al., 2001; Fontanier et al., 2002; Schönfeld et al., 2003). In contrast, assemblages of MIS 1, MIS 5e, the YD and the late terminations frequently contain miliolids (including *Pyrgo*), *B. mexicana*, *B. alazanensis*, and *Gyroidinoides* spp. and show low hBFAR values, thus suggesting reduced trophic conditions in those intervals (Murray, 2006).

While parallel trends across Terminations I and II are apparent along coordinate 1, both data-sets are well separated along coordinate 2 (Fig. 6). The contrasts in assemblage composition are most likely related to changes in oxygenation as well as the quantity and quality of available organic matter. However, the trends differ between glacial and stadial periods and those of interglacial and late termination periods. High abundances of deep infaunal taxa and low hBFAR values during MIS 2, HS 1, and the YD suggest a strong influence of depressed oxygenation on the faunal composition (culminating in HS 1), resulting in reduced specimen numbers. Peaks in the abundance of *M. pompilioides* during HS 1 and the YD are probably related to the increased input of refractory organic matter in these intervals (in HS 1, it is associated with a peak in IRD deposition; Poli et al., 2012). In contrast, the elevated hBFAR values (several times those of MIS 2) and high abundances of *B. marginata*, *B. aculeata*, *M. barleeanum*, and (in some samples) *U. pigmea* suggest high input of fresh, labile organic matter into the sediment during MIS 6 and most of HS 11 (Caralp, 1989; Fontanier et al., 2002). Most of those taxa are stress-tolerant and can survive variable

conditions of oxygenation and food. These conditions are only interrupted at the onset of HS 11 when a severe decrease in hBFAR, and peak abundances of *M. pompilioides* suggest increased input of refractory organic matter (Poli et al., 2012).

For the second group of samples, the assemblages of the late terminations are clearly separated from those of the BAIS, MIS 1 and (partly) MIS 5e. Highest miliolid abundances indicate a rapid improvement of oxygenation and oligotrophic conditions at the inception of interglacials. While high abundances of miliolids are maintained after the inception of MIS 5e, hyaline assemblages recover during MIS 1, resembling today's mesotrophic environment (see Section 5.1).

The long-term trends in deep-water temperature and oxygenation agree with and complement previous studies that link changes in local deep-water hydrography to changes in thermohaline circulation and the depth of the NEADW/LDW boundary during glacial/interglacial transitions. T_{dw} < 2 °C prevailed during MIS 2 and, most likely, HS 1. With the end of HS 1, T_{dw} remains above LGM levels. Decreased ventilation during MIS 2 is in agreement with AMOC reduced by ~30–40% during the LGM compared to the better ventilated MIS 1, and a stronger influence of southern sourced waters (Sarnthein et al., 2000; McManus et al., 2004; Lynch-Stieglietz et al., 2007). A period of particularly strong oxygen depletion is associated with HS 1 which supports views of a severe reduction or even shutdown of AMOC and maximum influence of southern sourced waters at this time (Skinner et al., 2003; McManus et al., 2004). During the early phase of the YD, oxygen depletion seems to have been less strong indicating that considerable NADW formation took place during this early stage despite ice rafting (Sarnthein et al., 2000). HS 1 and the YD share the input of refractory organic matter and a potential decrease in seasonality (tentatively indicated by *E. exigua*; see next paragraph), most likely the result of aged continental organic matter brought to the site during ice rafting. Trophic conditions at the sea-floor deteriorate from MIS 2 to MIS 1, paralleled by an increase in oxygenation heralding the establishment of present-day conditions.

Some notable differences occur between Termination I and Termination II. While HS 11 shares the input of refractory organic matter in its early stage with HS 1 and the YD (indicated by *M. pompilioides*), the persistently high abundances in *B. aculeata* and *B. marginata* indicate a generally elevated input of labile organic matter that culminates in the later phase of HS 11 with abundant *M. barleeanum* and high hBFAR values. This palaeoenvironmental trend is also recognized in trace fossil assemblages of the same interval (Rodríguez-Tovar et al., 2015). The increased input of organic matter coincides with a period of increased primary productivity along the western Iberian Margin during Termination II (Thomson et al., 2000). Food as a driving factor in contrast to oxygenation suggests a reduction of AMOC more similar to the YD and MIS 2 than HS 1 (Oppo et al., 1997). In the context of export productivity, low abundances of *E. exigua* potentially indicate seasonality is muted during MIS 6 and Termination II. It cannot be ruled out, however, that this is the result of an environment unfavourable for *E. exigua*, the exclusion of the fraction 63–125 μm or the reliance of *E. exigua* as sole indicator of seasonality (Schröder et al., 1987; Jorissen, 1999; Sun et al., 2006).

5.3. Limitations and potential of high-resolution records >212 μm

The restriction of foraminiferal analysis to coarse size fractions allows for the time-efficient acquisition of a large amount of data, and benthic foraminiferal studies in the area are generally based on size-fractions >250 μm (Caralp, 1987; Baas et al., 1998; Schönfeld et al., 2003). This approach puts further limitations on the interpretation in addition to the taphonomic effects, including the low number of shells, diminished species richness and diversity, and the loss of small-sized indicator species (Schröder et al., 1987; Fatela and Taborda, 2002; Schönfeld, 2012). The low-resolution data-sets offer an opportunity to evaluate these factors for the study area.

In Recent foraminiferal assemblages, only ~20% of foraminiferal taxa are represented in fractions >250 μm compared to the faunal inventory >63 μm, while ~75% are present in fractions >125 μm (Schönfeld, 2012). The result is an overrepresentation of certain species while small-sized taxa (including potentially important index taxa like *E. exigua*, bolivinids) are underrepresented or missing (Schröder et al., 1987). At U1385, abundances of *Pyrgo* spp., *Globobulimina* spp., *H. elegans*, *Melonis* spp., and *U. pigmea* are clearly over-emphasized in the larger size-fraction. In turn, *C. neoteretis*, *E. exigua*, *B. alazanensis*, and *Gyroidinoides* spp. are considerably underrepresented. As a result, potential indicators for T_{dw} and seasonality cannot be applied in the >212 μm data-sets and indicators for organic matter supply and oxygenation dominate these data-sets. The bias on assemblage composition is also evident in multivariate statistical analyses and has consequences for the interpretation. SIMPER and nMDS analyses clearly show that the combined fractions are primarily determined by the fraction 125–212 μm (contributing 75% to the total number of specimens in the combined fractions). As a consequence, the results for the smaller size-fraction are fairly similar to the combined fractions despite minor differences (Fig. 7). While *Globobulimina* spp. is slightly diminished, the separation along coordinate 1 is caused by the varying abundance of *C. neoteretis*, thus linked to deep-water temperature. Oxygenation might be the main component along coordinate 2, exemplified in the comparably increased abundances of miliolids in the YD sample resulting in its grouping in the nMDS analysis with samples from the inception of MIS 1 and MIS 5e.

As a consequence of the rare abundances of *C. neoteretis* >212 μm, the temperature signal is lost in the larger size-fraction, and nMDS coordinate 1 is determined by the antagonistic abundances of *Pyrgo* spp. and *Globobulimina* spp. reflecting mainly contrasts in food availability and oxygenation between glacial and interglacial periods (Fig. 7). Noteworthy, the oxygen depletion during HS 1 is particularly well expressed, whereas the YD shows more similarities to samples of MIS 1. The interpretation of coordinate 2 is less straightforward but might contain oxygenation as a component as indicated by varying abundances of deep infaunal taxa.

The application of the hBFAR proxy to coarse size-fractions also seems problematic as the considerably lowered number of hyaline shells per gram prohibits a meaningful interpretation (Fig. 3). Although the overall trend towards lower numbers from glacial to interglacial is preserved, short-term and minor changes cannot be resolved.

In summary, the >212 μm fraction of U1385 over-emphasizes the effect of oxygenation and food on the benthic microhabitat while the signal for deep-water temperature and seasonality is strongly diminished or lost entirely. hBFAR, while useful when size-fractions >125 μm are considered, cannot be applied due to low specimen numbers. The availability of the detailed records of U1385 thus clearly improve the interpretation of the high-resolution records of MD99-2334 K and MD01-2444 and their comparison to existing geochemical records.

5.4. Long- and short-term changes across Termination I

The foraminiferal records of U1385D and MD99-2334 K show parallels in long-term trends as well as differences most likely related to the different water depths. Similar to U1385D, the benthic foraminiferal record of MD99-2334 K is characterized by contrasting abundances of *Globobulimina* spp. and oxic indicators (cibicids, miliolids) during MIS 2 and MIS 1, indicating short- and long-term changes in deep-water ventilation. Rapid changes in the assemblages preceding HS 1 are essentially defined by the alternation of *Uvigerina* spp. and *Globobulimina* spp. dominance, suggesting relatively high organic carbon supply yet of different quality, and variable states of oxygenation (Schönfeld et al., 2003; Schönfeld and Altenbach, 2005). It appears that HS 3 and HS 2 both correspond to periods of relatively depressed oxygenation on the southwestern Iberian Margin. The frequent abundance of *Uvigerina* spp. during interstadial periods of MIS 2 is in stark contrast to U1385D where this species is virtually absent in the glacial samples. This contrast

between the two sites might be the result of different water depths as *U. pigmea*, the main component of *Uvigerina* spp., constitutes a major component of faunal assemblages from sites below 3000 m water depth in the area (Caralp, 1987; Schönfeld et al., 2003). The interval spanning HS 1, the BAIS, and the YD is characterized by the dominance of *Globobulimina* spp. (sometimes twice the abundance of U1385D). However, variations in the abundance of *Globobulimina* spp. during this interval indicate that ventilation changes occurred in parallel with HS 1, the BAIS and the YD, when local deep-water alternated between lower, higher, and again lower oxygenation states respectively, before the final transition to well-ventilated Holocene conditions. Short-term variations in oxygenation are indicated for both stadial periods. Maximum abundances of *Globobulimina* spp. in the early phase of HS 1 suggest significantly depressed oxygenation, while a slight decrease paralleled by a minor increase in hBFAR at U1385D indicates a more prominent role of export productivity in its later phase. A gradual decrease in deep-water oxygenation occurs over the YD interval, indicated by a final peak in *Globobulimina* spp. in its late phase.

Similar inferences regarding deep-water circulation changes recorded in MD99-2334 K have been made based on geochemical proxies for deep-water temperature (Skinner et al., 2003), radiometric dating (Skinner and Shackleton, 2004), and deep-water nutrient content (Skinner and Shackleton, 2006), all of which suggest an alternation between northern- and southern sourced deep-water masses across these millennial-scale events. In Fig. 9, geochemical proxies for T_{dw} (Mg/Ca of *G. affinis*; Skinner et al., 2003) and organic matter content ($\delta^{13}C_{benthic}$ of *C. wuellerstorfi*; Skinner and Shackleton, 2004) measured in MD99-2334 K are compared with the abundance of *Globobulimina* spp. There is a general correspondence between periods of reduced T_{dw}, lowered $\delta^{13}C_{benthic}$ and reduced oxygenation, suggesting that a deep-water circulation and/or sourcing signal may dominate all three records. The correspondence is particularly clear for the tripartite deglacial portion of the records, where both micropalaeontological and geochemical proxy records indicate transient changes in NE Atlantic deep-water circulation in parallel with HS 1, the BAIS and the YD.

The same may also be the case for faunal and geochemical variations associated with HS 3 and HS 2, although the correspondence of the proxy records is less clear for these events. In part, this is due to a paucity of $\delta^{13}C_{benthic}$ data, which in itself might indicate a severe limitation of the preferred oxygenated and/or oligotrophic microhabitat of *C. wuellerstorfi* (Altenbach et al., 1999). For better-resolved intervals of the $\delta^{13}C_{benthic}$ record however, distinct albeit fine-scaled mismatches with respect to the T_{dw} record can be identified, often in parallel with similar mismatches exhibited by the deep infaunal fauna. Hence at ~300 cm and ~240 cm depth, local maxima in both $\delta^{13}C_{benthic}$ and apparent oxygenation coincide with T_{dw} minima, rather than maxima as observed for the large-scale variations recorded in MD99-2334 K and as occurs in the modern deep Atlantic primarily as a result of deep-water circulation patterns (Broecker and Peng, 1982). Taken at face value, these mismatches may represent the occurrence of relatively cold, yet better-ventilated and low nutrient deep-water on the Iberian Margin. Alternatively, they might represent the effect of sedimentary time-averaging, resulting in the incorporation of *C. wuellerstorfi* and *Globobulimina* spp. specimens into the same sediment interval derived from short-lived periods of contrasting deep-water ventilation, lasting less than the residence time of the active sedimentation layer (perhaps ~400 years, given a sedimentation rate of ~20 cm/ka and the possibility of ~8 cm habitat penetration). Such averaging has been inferred for planktonic foraminifera (Skinner et al., 2003), and would require very rapid fluctuations in deep-water character (Corliss et al., 2002).

5.5. Long- and short-term changes across Termination II

Owing to their proximity, the records of U1385E and MD01-2444 show a high correspondence in their faunal trends and can be integrated easily (Hodell et al., 2013b). Similar to IODP Site U1385, the abundance records from core MD01-2444 show considerable differences to the data-sets of Termination I (Fig. 8). While interstadial conditions of MIS 6 resemble those of MIS 2 with the dominance of *Globobulimina* spp., their diminished abundances in most of HS 11 contrast stadials of Termination I. The high abundances of *Bulimina* spp. and *Melonis* spp. indicate increased food availability rather than oxygenation as the main factor during HS 11, particularly in the later stage of HS 11 and the transition into MIS 5e as indicated by elevated hBFAR values at U1385E-3H (Fig. 3). Geochemical proxy measurements performed in core MD01-2444, including T_{dw} (Mg/Ca of *G. affinis*) and organic matter content ($\delta^{13}C_{benthic}$ of *C. wuellerstorfi*; both Skinner and Shackleton, 2006), also reveal transient fluctuations in deep-water character across the penultimate glacial termination, and these are compared with the deep-infaunal taxa (Fig. 10). The geochemical and faunal proxies all co-vary across the oxygenation pulse at the onset of HS 11 IRD deposition, and therefore both indicate the occurrence of an early change in deep-water character in the NE Atlantic prior to the MIS 6/5e boundary. This deep-water circulation change was characterized by the increased influence of a warmer, more oxygenated water-mass depleted in organic matter (more suggestive of northern North Atlantic than Antarctic source).

In the later stage of HS 11 and the transition into MIS 5e, the relationship between the geochemical and faunal proxies is not obvious, with $\delta^{13}C_{benthic}$ and deep-infaunal taxa suggesting a later increase in deep-water ventilation than might be inferred from T_{dw} (Fig. 10). The first group of indices (indicating late oxygenation increase) are distinct from the latter proxy in that they can be significantly affected by organic matter input, with increased organic matter input allowing deep infaunal habitats to persist and providing a greater portion of $^{12}C/C$ for equilibration with the dissolved inorganic carbon (DIC) budget. A high

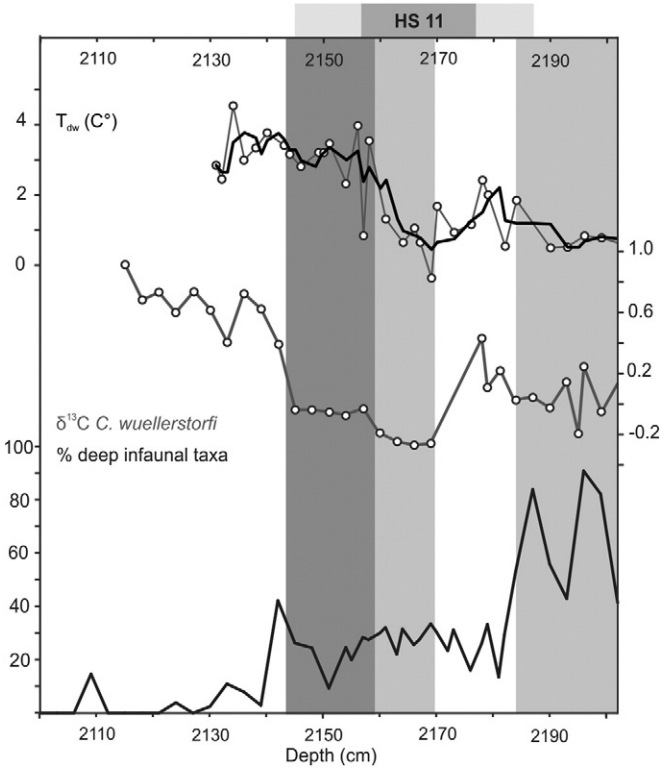

Fig. 10. Correlation of the abundance of deep-infaunal taxa (used as proxy of oxygen depletion) with existing geochemical records for deep-water temperature ($T_{dw;}$ calculated from Mg/Ca values of *G. affinis*; Skinner et al., 2003; Skinner and Shackleton, 2006) and benthic $\delta^{13}C$ (*C. wuellerstorfi*; Skinner and Shackleton, 2004, 2006) for MD01-2444. Light grey areas indicate intervals of low T_{dw}, dark grey interval indicates period of particularly high export productivity during HS 11.

supply of organic matter to the sea floor is suggested for this interval by the increase of *M. barleeanum* as well as strongly elevated hBFAR values at U1385E in the same interval (in contrast to HS 1). Organic matter exported from surface waters in sufficient quantity (perhaps due to a change in the seasonality of productivity pulses on the Iberian Margin; Thomson et al., 2000; Voelker and de Abreu, 2011) could have resulted in the release of ^{12}C into near-bottom water when eventually oxidized at the sea-floor, thus generating a "phytodetritus effect" in the $\delta^{13}C_{benthic}$ (Mackensen and Bickert, 1999; Zarriess and Mackensen, 2011).

The relationships illustrated in Fig. 10 are consistent with the existence of a "phytodetritus effect" during the latter half of HS 11, however they cannot unequivocally rule out an alternative interpretation of the geochemical and faunal census data, whereby a water-mass of similar T_{dw} to modern NEADW yet of relatively low oxygen and high organic matter content is inferred to have prevailed in the NE Atlantic at 2460 m depth across Termination II and into MIS 5e (Hodell et al., 2009; Galaasen et al., 2014). This persistent ambiguity underlines the difficulty of interpreting $\delta^{13}C$ data that necessarily includes a deep-water source signature, is subsequently altered by deep-water transit through the ocean, and potentially bears an additional local organic carbon respiration imprint (Zarriess and Mackensen, 2011). The NE Atlantic margin is particularly problematic in this regard, being characterized by high upwelling productivity and the admixture of deep-waters derived from both southern and northern sources (Van Aken, 2000; Voelker and de Abreu, 2011).

6. Conclusions

The integration of census counts of benthic foraminifera from low-resolution records >125 μm of IODP Site U1385 with high-resolution records >212 μm of sites MD99-2334 K and MD01-2444 allows for a detailed analysis of changes in deep-water hydrography along the SW Iberian Margin across Terminations I and II. The evaluation of the size-fraction 125–212 μm, missing in previous studies in the area, provides information about potential biases on the interpretation of the microfossil records from taphonomic processes and the use of restricted size-fractions. The comparison of recent (mudline) and fossil assemblages indicates the quick post-mortem disintegration of shells of astrorhizoid taxa, which make up ~80% of present-day fauna, resulting in impoverished fossil assemblages at IODP Site U1385. A straightforward application of quantitative proxy methods (e.g., BFAR, BFOI) is problematic under these circumstances, and they should be modified (e.g., the herein introduced hBFAR) or abandoned. However, the taphocoenoses still carry a qualitative palaeoenvironmental signal that is most fully expressed in the 125–212 μm size-fraction, but nonetheless also expressed to some degree in the >212 μm size-fraction.

Elevated trophic conditions and considerable fluctuations in oxic conditions characterize MIS 2 and Termination I, with minima oxygenation culminating in the YD and HS 1, 2 and 3. The coincidence of low oxic conditions with decreased water-temperature (Mg/Ca) and lowered benthic $\delta^{13}C$ indicates the strong influence of a southern sourced water-mass during these periods. HS 1 is the most extreme of these intervals, providing further evidence for a severe temporary reduction or even shutdown of AMOC. With the inception of MIS 1, organic matter supply at the sea-floor decreases and a better ventilated deep-water environment bathed by NEADW is established.

Severe alterations of deep-water conditions are also occurring at the penultimate termination. The temporary incursion of a NADW-like water-mass prior to HS 11 is suggested by faunal and geochemical data. Clear indications of southern-sourced water are limited to the early phase of HS 11, whereas the later part of the stadial was marked by increased input of organic matter, potentially explaining the decoupling of benthic $\delta^{13}C$ and Mg/Ca records of earlier studies as a "phytodetritus effect" on the carbon isotope signal. However, the presence of a warm, nutrient-rich and poorly oxygenated water-mass cannot be discarded. Similar to Termination I, food supply at the sea-floor decreases with the inception of interglacial MIS 5e, paralleled by increased NEADW production.

This study demonstrates the potential application of assemblage analysis to fossil foraminiferal faunas for inferring palaeoenvironmental conditions, provided limitations caused by taphonomy and size-fractions are considered. The interpretation of high-resolution records >212 μm benefit considerably from the integration with a detailed evaluation of the complete faunal inventory >125 μm at a lower resolution, thereby providing a robust tool for the reconstruction of deep-water change in the North Atlantic. Multiproxy comparisons of micropalaeontological and geochemical records can be essential to evaluate a given proxy's environmental significance, and to identify specific secondary controls on proxy measurements.

Supplementary data to this article can be found online at http://dx.doi.org/10.1016/j.gloplacha.2015.06.002.

Acknowledgements

Sample material for this study has been provided by the Integrated Ocean Drilling Program, and the micropalaeopalaeontological team of IODP Expedition 339 is thankfully acknowledged for its help with mudline sampling. Antje Voelker (Instituto Português do Mar e da Atmosfera, Lisbon, Portugal) and Michael Sarnthein (Universität Innsbruck, Austria) are acknowledged for helpful discussions. The constructive comments of two anonymous reviewers helped to improve the original manuscript. L.S. is grateful for the support of N.J. Shackleton, which permitted the acquisition of the high-resolution data included in this study. This study was financially supported through Exchange Visit Grant 4455 of the ESF Research Networking Programmes to P.G., NERC Grant NE/K005804/1 to D.H. and L.S., and contributes to project P25831-N29 of the Austrian Science Fund (FWF).

Appendix A

The herein applied taxonomic concepts generally follow the widely used reference works on deep-sea benthic foraminifera by Van Morkhoven et al. (1986), Jones (1994) and Holbourn et al. (2013). The revised taxonomic concepts of Seidenkrantz (1995) and Schönfeld (2006) have been applied to *Cassidulina* and the *Uvigerina*, respectively. The identification of *Cassidulina neoteretis* is primarily based on its non-serrate apertural plate (Seidenkrantz, 1995).

In the following, specific references to plates and figures are listed that have been used for the identification of the most common foraminiferal species of this study (also see Plate 1):

Bulimina aculeata d'Orbigny, 1826: Holbourn et al. (2013), p. 88, Figs. 1–3.
Bulimina alazanensis Cushman, 1927: Holbourn et al. (2013), p. 90, Figs. 1–2.
Bulimina marginata d'Orbigny, 1826: van Morkhoven et al. (1986), Pl. 2, Figs. 1
Bulimina mexicana Cushman, 1922: Holbourn et al. (2013), p. 110, Figs. 1–2.
Cassidulina neoteretis Seidenkrantz, 1995: Seidenkrantz (1995), Pl. 2, 1–14; Pl. 3, Figs. 1–8.
Chilostomella oolina Schwager, 1878: Holbourn et al. (2013), p. 148, Figs. 1–2.
Epistominella exigua (Brady, 1884): Jones (1994), Pl. 103, Fig. 14
Globobulimina affinis (d'Orbigny, 1839): Cushman (1922), Pl. 20. Fig. 6
Globocassidulina minuta (Cushman, 1933): Arellano et al. (2011), Pl. 4, Fig. 5
Gyroidinoides soldanii (d'Orbigny, 1826): Jones (1994), Pl. 107, Fig. 7

Hoeglundina elegans (d'Orbigny, 1878): van Morkhoven et al. (1086), Pl. 29, Figs. 1–2.
Melonis barleeanum (Williamson, 1858): Holbourn et al. (2013), p. 354, Figs. 1–2.
Melonis pompilioides (Fichtel and Moll, 1798): Jones (1994), Pl. 108, Fig. 10
Pyrgo murrhina (Schwager, 1866): Jones (1994), Pl. 2, Figs. 11, 15
Saccorhiza ramosa (Brady, 1879): Jones (1994), Pl, Figs. 15–19.
Sigmoilopsis schlumbergeri (Silvestri, 1904): Jones (1994), Pl. 8. Figs. 1–4.
Uvigerina pigmea d'Orbigny, 1826: Schönfeld (2006), Pl.1, Figs. 1–6.

References

Altenbach, A.V., Pflaumann, U., Schiebel, R., Thies, A., Timm, S., Trauth, M., 1999. Scaling percentages and distributional patterns of benthic foraminifera with flux rates of organic carbon. J. Foraminifer. Res. 29, 173–185.

Baas, J.H., Schönfeld, J., Zahn, R., 1998. Mid-depth oxygen drawdown during Heinrich events: evidence from benthic foraminiferal community structure, trace-fossil tiering, and benthic $\delta^{13}C$ at the Portuguese Margin. Mar. Geol. 152, 25–55.

Broecker, W.S., Peng, T.-H., 1982. Tracers in the Sea. Lamont-Doherty Earth Observatory, Columbia University (702 pages).

Caralp, M.-H., 1987. Deep-sea circulation in the northeastern Atlantic over the past 30 000 years: the benhic foraminiferal record. Oceanol. Acta 10, 27–40.

Caralp, M.-H., 1989. Abundance of *Bulimina exilis* and *Melonis barleeanum*: relationship to the quality of marine organic matter. Geo-Mar. Lett. 9, 37–43.

Corliss, B.H., McCorkle, D.C., Higdon, D.M., 2002. A time series study of the carbon isotopic composition of deep-sea benthic foraminifera. Paleoceanography 17, 1036.

Cushman, 1922. The foraminifera of the Atlantic Ocean. Part 3, Textulariidae. Bull. US Natl Mus. 104, 1–149.

Expedition 339 Scientists, 2013. Site U1385. In: Stow, D.V.A., Hernandez-Molina, F.J., Alvarez Zarikian, C.A., the Expedition 339 Scientists (Eds.), Proceedings of IODP, p. 339. http://dx.doi.org/10.2204/iodp.proc.339.103.2013 (Tokyo).

Fatela, F., Taborda, R., 2002. Confidence limits of species proportions in microfossil assemblages. Mar. Micropalaeontol. 45, 169–174.

Fontanier, C., Jorissen, F.J., Licari, L., Alexandre, A., Anschutz, P., Carbonel, P., 2002. Live benthic foraminiferal faunas from the Bay of Biscay: faunal density, composition, and microhabitats. Deep-Sea Res. I 49, 751–785.

Galaasen, E.V., Ninnemann, U.S., Irvali, N., Kleiven, H.F., Rosenthal, Y., Kissel, C., Hodell, D.A., 2014. Rapid reductions in North Atlantic Deep Water during the peak of the Last Interglacial Period. Science 343, 1129–1132.

Goldstein, S.T., Barker, W.W., 1988. Test ultrastructure and taphonomy of the monothalamous agglutinated foraminifer *Cribrothalammina*, n.gen., *alba* (Heron-Allen and Earland). J. Foraminifer. Res. 18, 130–136.

Gooday, A.J., Rathburn, A.E., 1999. Temporal variability in living deep-sea benthic foraminifera: a review. Earth Sci. Rev. 46, 187–212.

Griveaud, C., Jorissen, F., Anschutz, P., 2010. Spatial variability of live benthic foraminiferal faunas on the Portuguese margin. Micropaleontology 56, 297–322.

Hammer, Ø., 2012. PAST—palaeontological statistics, version 2.17. Reference Manual (229 pages. http://www.nhm2.uio.no/norlex/past/pastmanual.pdf).

Hammer, Ø., Harper, D.A.T., Ryan, P.D., 2001. PAST: palaeontological statistics software package for education and data analysis. Palaeontol. Electron. 4 (http://palaeo-electronica.org/2001_1/past/issue1_01.htm).

Herguera, J.C., Berger, W.H., 1991. Palaeoproductivity from benthic foraminifera abundance: glacial to postglacial change in the west-equatorial Pacific. Geology 19, 1173–1176.

Hernández-Molina, F.J., Serra, N., Stow, D.A.V., Llave, E., Ercilla, G., Van Rooij, D., 2011. Along-slope oceanographic processes and sedimentary products around the Iberian Margin. Geo-Mar. Lett. 31, 315–341.

Hodell, D.A., Channell, J.E.T., Curtis, J.H., Romero, O.E., Roehl, U., 2008. Onset of "Hudson Strait" Heinrich events in the eastern North Atlantic at the end of the middle Pleistocene transition (~640 ka)? Paleoceanography 23, PA4128.

Hodell, D.A., Minth, E.K., Crutis, J.H., McCave, I.N., Hall, I.R., Channell, J.E.T., Xuan, C., 2009. Surface and deep-water hydrography on Gardar Drift (Iceland Basin) during the last interglacial period. Earth Planet. Sci. Lett. 288, 10–19.

Hodell, D., Crowhurst, S., Skinner, L., Tzedakis, P.C., Margari, V., Channell, J.E.T., Kamenov, G., Maclachlan, S., Rothwell, G., 2013a. Response of Iberian Margin sediments to orbital and suborbital forcing over the past 420 ka. Paleoceanography 28, 185–199.

Hodell, D., Lourens, L., Stow, D.A.V., Hernández-Molina, J., Alvarez Zarikian, C.A., Shackleton Site Project Managers, 2013b. The "Shackleton Site" (IODP Site U1385) on the Iberian Margin. Sci. Drill. 16, 13–19.

Holbourn, A., Henderson, A.S., Macleod, N., 2013. Atlas of benthic foraminifera. Wiley–Blackwell (654 pages).

Jones, R.W., 1994. The Challenger Foraminifera. Oxford University Press (149 pages).

Jorissen, F.J., 1999. Benthic foraminiferal successions across Late Quaternary Mediterranean sapropels. Mar. Geol. 153, 91–101.

Jorissen, F., 2003. Benthic Foraminiferal Microhabitats Below the Sediment–water Interface. In: SenGupta, B.K. (Ed.), Modern foraminifera. Kluwer Academic Publishers, pp. 161–179.

Jorissen, F.J., De Stigter, H.C., Widmark, J.G.V., 1995. A conceptual model explaining benthic foraminiferal microhabitats. Mar. Micropalaeontol. 22, 3–15.

Jorissen, F.J., Fontanier, C., Thomas, E., 2007. Palaeoceanographical proxies based on deep-sea benthic foraminiferal assemblage characteristics. In: Hillaire-Marcel, C., de Vernal, A. (Eds.), Proxies in Late Cenzoic Palaeoceanography: Pt. 2: Biological tracers and biomarkers. Elsevier, pp. 263–325.

Kaiho, K., 1999. Effect of organic carbon flux and dissolved oxygen on the benthic foraminiferal oxygen index (BFOI). Mar. Micropalaeontol. 37, 67–76.

Kuhnt, W., Collins, E., Scott, D.B., 2000. Deep water agglutinated foraminiferal assemblages across the Gulf Stream: distribution patterns and taphonomy. In: Hart, M.B., Kaminski, M.A., Smart, C.W. (Eds.), Proceedings of the Fifth International Workshop on Agglutinated Foraminifera. Grzybowski Foundation Special Publication 7, pp. 261–298.

Lejzerowicz, F., Esling, P., Majewski, W., Szczucinski, W., Decelle, J., Obadia, C., Martinez Arbizu, P., Pawlowski, J., 2013. Ancient DNA complements microfossil record in deep-sea subsurface sediments. Biol. Lett. 9, 20130283.

Lynch-Stieglitz, J., Adkins, J.F., Curry, W.B., Dokken, T., Hall, I.R., Herguera, J.C., Hirschi, J.J.-M., Ivanova, E.V., Kissel, C., Marchal, O., Marchitto, T.M., McCave, I.N., McManus, J.F., Mulitza, S., Ninnemann, U., Peeters, F., Yu, E.-F., Zahn, R., 2007. Atlantic meridional overturning during the last glacial maximum. Science 316, 66–69.

Mackensen, A., Bickert, T., 1999. Stable carbon isotopes of surface sediments. In: Fischer, G., Wefer, G. (Eds.), Use of Proxies in Paleoceanography — Examples from the South Atlantic. Spinger, Berlin, Heidelberg, pp. 229–254.

Mackensen, A., Hald, M., 1988. *Cassidulina teretis* Tappan and *C. laevigata* D'Orbigny: their modern and late quaternary distribution in northern seas. J. Foraminifer. Res. 18, 16–24.

Mackensen, A., Sejrup, H.P., Jansen, E., 1985. The distribution of living benthic foraminifera on the continental slope and rise off Southwest Norway. Mar. Micropalaeontol. 9, 275–306.

Margari, V., Skinner, L.C., Hodell, D.A., Martrat, B., Toucanne, S., Grimalt, J.O., Gibbard, P.L., Lunkka, J.P., Tzedakis, P.C., 2014. Land-ocean changes on orbital and millennial time scales and the penultimate glaciation. Geology 42, 183–186.

McManus, J.F., Francois, R., Gherardi, J.-M., Keigwin, L.D., Brown-Leger, S., 2004. Collapse and rapid resumption of Atlantic meridional circulation linked to deglacial climate changes. Nature 428, 834–837.

Morigi, C., Jorissen, F.J., Gervais, A., Guichard, S., Borsetti, A.M., 2001. Benthic foraminiferal faunas in surface sediments off NW Africa: relationship with the organic flux to the ocean floor. J. Foraminifer. Res. 31, 350–368.

Murray, J.W., 2006. Ecology and Applications of Benthic Foraminifera. Cambridge University Press, Cambridge (426 pages).

Oppo, D.W., Horowitz, M., Lehmann, S.J., 1997. Marine core evidence for reduced deep water production during Termination II followed by a relative stable substage 5e (Eemian). Paleoceanography 12, 51–63.

Phipps, M., Jorissen, F., Pusceddu, A., Bianchelli, S., De Stigter, H., 2012. Live benthic foraminiferal faunas along a bathymetrical transect (282–4987 m) on the Portuguese margin (NE Atlantic). J. Foraminifer. Res. 42, 66–81.

Piña-Ochoa, E., Høgslund, S., Geslin, E., Cedhagen, T., Revsbech, N.P., Nielsen, L.P., Schweizer, M., Jorissen, F., Rysgaard, S., Risgaard-Petersen, N., 2010. Widespread occurrence of nitrate storage and denitrification among Foraminifera and *Gromiida*. PNAS 107, 1148–1153.

Poli, M.S., Meyers, P.A., Thunell, R.C., Capodivacca, M., 2012. Glacial-interglacial variations in sediment organic carbon accumulation and benthic foraminiferal assemblages on the Bermuda Rise (ODP Site 1063) during MIS 13 to 10. Paleoceanography 27, PA3216.

Rodríguez-Tovar, F.J., Dorador, J., Grunert, P., Hodell, D., 2015. Deep-sea trace fossil and benthic foraminiferal assemblages across glacial Terminations 1, 2 and 4 at the "Shackleton Site" (IODP Expedition 339). Global and Planetary Change. http://dx.doi.org/10.1016/j.gloplacha.2015.05.003.

Sarnthein, M., Stattegger, K., Dreger, D., Erlenkeuser, H., Grootes, P., Haupt, B., Jung, S., Kiefer, T., Kuhnt, W., Pflaumann, U., Schaefer-Neth, C., Schulz, Hartmut, Schulz, M., Seidov, D., Simstich, J., van Kreveld, S., Vogelsang, E., Voelker, A., Weinelt, M., 2000. Fundamental Modes and Abrupt Changes in North Atlantic Circulation and Climate over the last 60 ky—Concepts, Reconstruction and Numerical Models. In: Schaefer, P., Ritzrau, W., Schlueter, M., Thiede, J. (Eds.), The Northern North Atlantic: A Changing Environment. Springer, Berlin, pp. 365–410.

Schönfeld, J., 2001. Benthic foraminifera and pore-water oxygen profiles: a re-assessment of species boundary conditions at the western Iberian Margin. J. Foraminifer. Res. 31, 86–107.

Schönfeld, J., 2006. Taxonomy and distribution of the *Uvigerian peregrina* plexus in the tropical to northeastern Atlantic.

Schönfeld, J., 2012. History and development of methods in Recent benthic foraminiferal studies. J. Micropalaeontol. 31, 53–72.

Schönfeld, J., Altenbach, A.V., 2005. Last glacial to recent distribution pattern of deep-water Uvigerina species in the north-eastern Atlantic. Mar. Micropalaeontol. 57, 1–24.

Schönfeld, J., Zahn, R., 2000. Late Glacial and Holocene history of the Mediterranean Outflow. Evidence from benthic foraminiferal assemblages and stable isotopes at the Portuguese margin. Palaeogeogr. Palaeoclimatol. Palaeoecol. 159, 85–111.

Schönfeld, J., Zahn, R., de Abreu, L., 2003. Surface and deep water response to rapid climate changes at the Western Iberian Margin. Glob. Planet. Chang. 36, 237–364.

Schröder, C.J., 1988. Subsurface preservation of agglutinated foraminifera in the northwest Atlantic Ocean. Abh. Geol. Bundesanst. 41, 325–336.

Schröder, C.J., Scott, D.B., Meioli, F.S., 1987. Can smaller benthic foraminifera be ignored in paeloenvironmental analyses? J. Foraminifer. Res. 17, 101–105.

Schröder-Adams, C.J., van Rooyen, D., 2011. Response of Benthic foraminiferal assemblages to contrasting environments in Baffin Bay and the Northern Labrador Sea, Northwest Atlantic. Arctic 64, 317–341.

Seidenkrantz, M.-S., 1995. *Cassidulina teretis* and *Cassidulina neoteretis* new species (Foraminifera): stratigraphic markers for deep sea and outer shelfs. J. Micropalaeontol. 14, 145–157.
Shackleton, N., Hall, M.A., Vincent, E., 2000. Phase relationships between millennial-scale events 64,000–24,000 years ago. Paleoceanography 15, 565–569.
Skinner, L., Elderfield, H., 2007. Rapid fluctuations in the deep North Atlantic heat budget during the last glacial period. Paleoceanography 22, PA1205.
Skinner, L.C., McCave, I.N., 2003. Analysis and modeling of gravity- and piston coring based on soil mechanics. Mar. Geol. 199, 181–204.
Skinner, L., Shackleton, N., 2004. Rapid transient changes in the northeast Atlantic deep water ventilation age across Termination I. Paleoceanography 19, PA2005.
Skinner, L.C., Shackleton, N., 2006. Deconstructing Terminations I and II: revisiting the glacioeustatic paradigm based on deep-water temperature estimates. Quat. Sci. Rev. 25, 3312–3321.
Skinner, L., Shackleton, N., Elderfield, H., 2003. Millenial/scale variability of deep-water temperature and $\delta^{18}O_{dw}$ indicating deep-water source variations in the Northeast Atlantic, 0–34 cal. ka BP. Geochem. Geophys. Geosyst. 4. http://dx.doi.org/10.1029/2003GC000585.
Sun, X., Corliss, B.H., Brown, C.W., Showers, W.J., 2006. The effect of primary productivity and seasonality on the distribution of deep-sea benthic foraminifera in the North Atlantic. Deep-Sea Res. I 53, 28–47.
Thomson, J., Nixon, S., Summerhayes, C.P., Rohling, E.J., Schönfeld, J., Zahn, R., Grootes, P., Abrantes, F., Gaspar, L., Vaqueiro, S., 2000. Enhanced productivity on the Iberian margin during glacial/interglacial transitions revealed by barium and diatoms. J. Geol. Soc. 157, 667–677.
Van Aken, H.M., 2000. The hydrography of the mid-latitude northeast Atlantic Ocean I: the deep water masses. Deep-Sea Res. I 47, 757–788.
Van Morkhoven, F.P.C.M., Berggren, W.A., Edwards, A.S., 1986. Cenozoic cosmopolitan deep-water benthic foraminifera. Elf-Aquitaine Mem. 11 (423 pages).
Voelker, A.H.L., de Abreu, L., 2011. A review of abrupt climate change events in the Northeastern Atlantic Ocean (Iberian Margin): Latitudinal, Longitudinal, and Vertical Gradients. Abrupt Climate Change: Mechanisms, Patterns, and Impacts. Geophysical Monograph Series 193. American Geophysical Union, Washington D.C., pp. 15–37.
Williamowski, R., Zahn, R., 2000. Upper ocean circulation in the glacial North Atlantic from benthic foraminiferal isotope and trace element fingerprinting. Paleoceanography 15, 515–527.
Zarriess, M., Mackensen, A., 2011. Testing the impact of seasonal phytodetritus deposition on $\delta^{13}C$ of epibenthic foraminifera *Cibicidoides wuellerstorfi*: A 31,000 year high-resolution record from the northwest African continental slope. Paleoceanography 26, PA2202.